◆ Human Brain Mapping 38:3899–3916 (2017) ◆

Resting State Functional Connectivity of the Ventral Auditory Pathway in Musicians with Absolute Pitch

Seung-Goo Kim* and Thomas R. Knösche

Research Group for MEG and EEG — Cortical Networks and Cognitive Functions, Max Planck Institute for Human Cognitive and Brain Sciences, Leipzig, Germany

Abstract: Absolute pitch (AP) is the ability to recognize pitch chroma of tonal sound without external references, providing a unique model of the human auditory system (Zatorre: Nat Neurosci 6 (2003) 692–695). In a previous study (Kim and Knösche: Hum Brain Mapp (2016) 3486–3501), we identified enhanced intracortical myelination in the right planum polare (PP) in musicians with AP, which could be a potential site for perceptional processing of pitch chroma information. We speculated that this area, which initiates the ventral auditory pathway, might be crucially involved in the perceptual stage of the AP process in the context of the "dual pathway hypothesis" that suggests the role of the ventral pathway in processing nonspatial information related to the identity of an auditory object (Rauschecker: Eur J Neurosci 41 (2015) 579–585). To test our conjecture on the ventral pathway, we investigated resting state functional connectivity (RSFC) using functional magnetic resonance imaging (fMRI) from musicians with varying degrees of AP. Should our hypothesis be correct, RSFC via the ventral pathway is expected to be stronger in musicians with AP, whereas such group effect is not predicted in the RSFC via the dorsal pathway. In the current data, we found greater RSFC between the right PP and bilateral anteroventral auditory cortices in musicians with AP. In contrast, we did not find any group difference in the RSFC of the planum temporale (PT) between musicians with and without AP. We believe that these findings support our conjecture on the critical role of the ventral pathway in AP recognition. *Hum Brain Mapp 38:3899–3916, 2017.*

Key words: absolute pitch; pitch chroma perception; human auditory system; planum polare; dual auditory pathway hypothesis; functional magnetic resonance imaging; resting-state network

INTRODUCTION

Previous Neuroimaging Studies on Absolute Pitch

Absolute pitch (AP) is the ability to recognize the pitch of any given tonal sound without external reference [Miyazaki, 1988], which can be behaviorally observed by verbal labeling and/or reproducing the pitch. For more than a century this variant of pitch perception has drawn psychologists' attention because it provides a unique model of the human auditory system that allows us to investigate the interaction of genetic and developmental factors

Additional Supporting Information may be found in the online version of this article.

*Correspondence to: Seung-Goo Kim, Stephanstraße 1A, 04103 Leipzig, Germany. E-mail: sol@snu.ac.kr

Received for publication 12 January 2017; Revised 6 April 2017; Accepted 23 April 2017.

DOI: 10.1002/hbm.23637

Published online 8 May 2017 in Wiley Online Library (wileyonlinelibrary.com).

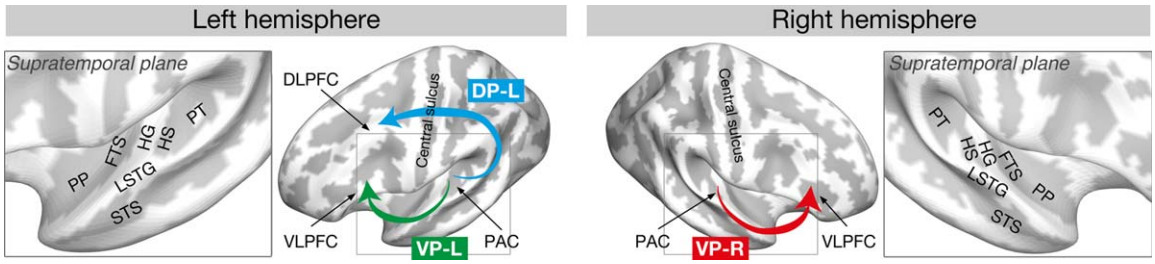

Figure 1.

Brain regions related to AP processing. Abbreviations: DP-L, left dorsal pathway; DLPFC, dorsolateral prefrontal cortex; FTS, first transverse sulcus; HG, Heschl's gyrus; HS, Heschl's sulcus; LSTG, lateral superior temporal gyrus; PP, planum polare; PT, planum temporale; STS, superior temporal sulcus; VLPFC, ventrolateral prefrontal cortex; VP-L, left ventral pathway; VP-R, right ventral pathway. [Color figure can be viewed at wileyonlinelibrary.com]

[Meyer, 1899; Zatorre, 2003]. The likelihood of developing AP was reported to increase when there are other AP listeners in the family and when the age of one's first formal musical training is earlier than 6 years [Baharloo et al., 1998, 2000].

A number of behavioral studies reported that AP listeners are not better than non-AP listeners in identifying pitch height (i.e., octave index), whereas AP listeners are highly accurate in identifying pitch chroma (i.e., one of the twelve tones constituting an octave in the Western music scale), suggesting that "absolute pitch" is in fact "absolute pitch chroma" [Deutsch, 2013; Deutsch and Henthorn, 2004; Kim and Knösche, 2016; Miyazaki, 1988; Takeuchi and Hulse, 1993]. Pitch chroma can be seen as a discretization of continuous frequency. While non-AP listeners perceive pitch chroma only in a relative way, based on tonal context (thus tonal function of the pitch) or an external reference (similarity perception of octave-spaced tones), AP listeners have been reported to directly perceive pitch chroma "in a similar fashion to categorization of phonemes" [Siegel, 1974].

By intuition, a natural conception of the mechanism underlying AP would comprise two distinct sub-processes [Levitin, 2004; Levitin and Rogers, 2005; Schulze et al., 2013]: the categorization in pitch chroma ("perceptual process") and the verbal/nonverbal labeling of the perceived pitch chroma ("associative process"). The idea of segregation and integration of these two processes has constituted the general framework of many neuroimaging studies. Structural and functional differences in the auditory cortex were interpreted as evidence for the perceptual process, whereas findings in the frontal lobe were related to the associative process. For instance, a greater volume of right Heschl's gyrus (HG) [Wengenroth et al., 2014] was interpreted as a signature of enhanced perceptual processing involved in AP recognition, because the medial part of HG is included in the primary auditory cortex (PAC) [Griffiths and Hall, 2012].

Theories on auditory perception are often based on the "dual auditory stream" hypothesis, which postulates that the dorsal auditory pathway including the planum temporale (PT) mostly processes spatial information of an auditory object (blue arrow in Fig. 1), whereas the ventral auditory pathway including the planum polare (PP) processes properties of an auditory object that are not dependent upon spatial location (green and blue arrows in Fig. 1) [Arnott et al., 2004; Kaas and Hackett, 1999; Kusmierek and Rauschecker, 2009; Rauschecker, 2015; Rauschecker and Tian, 2000; Tian et al., 2001; Warren and Griffiths, 2003; Warren et al., 2003a]. Of most relevance in the present context, Warren and colleagues demonstrated higher sensitivity to pitch chroma in the PP and higher sensitivity to pitch height in the PT [Warren et al., 2003b]. As mentioned above, the processing of pitch chroma is the essential characteristic of AP [Deutsch, 2013; Deutsch and Henthorn, 2004; Kim and Knösche, 2016; Miyazaki, 1988; Takeuchi and Hulse, 1993], which speaks for a specific involvement of the ventral pathway in AP perception, most probably in the early perceptual process. This has been corroborated by the finding of increased intra-cortical myelination in the right PP of AP possessors [Kim and Knösche, 2016]. Moreover, cortical thickness and BOLD auditory response in ventrolateral prefrontal cortex (VLPFC), which is also part of the ventral pathway, has been implicated in previous studies [Bermudez et al., 2009; Dohn et al., 2015; Wengenroth et al., 2014].

However, other aspects of AP processing seem to be also supported by the fronto-temporal network of the dorsal pathway. For example, a smaller surface area (or a smaller volume) of the right PT [Keenan et al., 2001; Schlaug et al., 1995; Wilson et al., 2009] and greater hemodynamic activation in the left PT during passive listening to musical tones were found in musicians with AP [Wilson et al., 2009]. Because the PT is known as an important non-primary auditory cortex in relation to pitch salience [Griffiths and Warren, 2002; Hall and Plack, 2009], this was interpreted as being involved in the "perceptual process." In addition, greater BOLD activation in musicians with AP was found in the left dorsolateral prefrontal cortex (DLPFC) [Zatorre et al., 1998]. Because the DLPFC was also found to be correlated with learning associations between a verbal label and musical harmony [Bermudez

and Zatorre, 2005], it was suggested to be involved in the "associative process." Moreover, integration of the two processes was demonstrated by phase coupling between the source activities of the DLPFC and superior temporal gyrus (STG), which were reconstructed from electroencephalography (EEG) data [Elmer et al., 2015] and by greater fractional anisotropy (FA; an index of the directionality of a diffusion tensor) of the superior longitudinal fasciculus (SLF) [Oechslin et al., 2009], an important axonal connection of the dorsal auditory pathway.

Absolute Pitch Specific Microarchitecture in the Right Planum Polare

While previous *in vivo* findings strongly suggest that a fronto-temporal network supports the AP process, details of the actual neural implementation of AP remain undiscovered. In this context, cortical microarchitecture, which reflects functional organization of cortical columns [Nieuwenhuys, 2013], might play an important role. In our previous study [Kim and Knösche, 2016], we investigated the myeloarchitecture of the cortex of musicians with and without AP, utilizing quantitative T1 mapping with an ultra-high field (7 T) magnetic resonance imaging (MRI) [Geyer et al., 2011; Marques and Gruetter, 2013]. We identified a specific area in the right planum polare (PP) that exhibited heavier intracortical myelination in AP as compared to non-AP musicians. This difference was only found at mid-cortical depth, implicating that the denser myelination might be related to tangential intracortical fibers rather than long-range connections through the white matter. Thus, the increased myelination might reflect enhanced local connectivity. Importantly, this area was close to, but spatially distinct from, another area in anterolateral HG, which was strongly myelinated for subjects with superior frequency discrimination ability. In the PP cortex, the cell density in layer III is greater than in the lateral STG, but smaller than in the PAC. Accordingly, this area may be considered as one of the nonprimary auditory cortices involved in relatively early stages of cortical acoustic processing [Rivier and Clarke, 1997]. A recent diffusion spectrum imaging (DSI) study in normal human brains reported a strong interconnection between the PAC and the anterior auditory (AA) area, which is a subregion of the PP [Cammoun et al., 2014].

Motivation for Resting-State fMRI and Hypotheses

In the current study, we test an involvement of the ventral pathway in AP recognition, and in particular the highly myelinated area in the right PP, using resting state functional MRI data (rs-fMRI). This type of data has been extensively used in the context of the "human connectome" [Van Essen et al., 2012]. Spontaneous activity during rest, without a particular instruction, is believed to be reflective of structural and intrinsic functional connectivity, which is built during development and may be modified by Hebbian rules [Smith et al., 2009; Yeo et al., 2015]. In previous rs-fMRI studies, distinguishable patterns of resting-state functional connectivity (RSFC) were related to behavioral and cognitive characteristics such as musical practice [Fauvel et al., 2014; Luo et al., 2012] and motor sequence learning [Bonzano et al., 2015]. We therefore expect RSFC, particularly of the auditory cortex, to reflect AP recognition abilities.

We hypothesize that if the increased local connectivity in the right PP (as indexed by increased intracortical myelination) is relevant for AP, then this region should exhibit greater RSFC with (1) adjacent auditory cortices, (2) homologous auditory regions in the left hemisphere, and (3) the left hemisphere fronto-temporal network. The rationale of our hypotheses is as follows:

1. Given that cortical myelin would provide additional electric insulation and decrease local transmission times, it may increase efficiency and specificity of information transfer. Consequently, neural communication via intracortical connections would benefit from the myelination of local circuits. Therefore, we expect greater short-range RSFC of the right PP with neighboring auditory cortex (AC) areas in individuals with more accurate AP perception. A similar link between local morphology (local gray matter volume) and RSFC was recently found in the left STG in musicians compared to nonmusicians [Fauvel et al., 2014].
2. Studies using independent component analysis (ICA) based methods have consistently shown that the auditory RSN bears high modularity within bilateral supratemporal planes (STPs), including HG, HS, the PP, and PT, both in general populations [Damoiseaux et al., 2006; Shirer et al., 2012; Smith et al., 2009, 2012, 2013] and musicians [Fauvel et al., 2014; Luo et al., 2012]. Additionally, in a histological study with rhesus monkeys [Pandya et al., 1969], the PAC and the posterior part of the STP were found to be structurally connected to their contralateral homologs via the corpus callosum, whereas the anterior parts of the STPs were connected via the anterior commissure. This line of evidence suggests high interhemispheric functional connectivity (FC) between the homologous auditory regions. As mentioned above, the ventral auditory pathway is likely to process pitch chroma, that is, nonspatial information [Warren et al., 2003a]. Therefore, it can be expected that the left PP in an individual with proficient AP would also be involved in nonspatial information processing, which the right PP undertakes. This could result in increased interhemispheric FC between two homologous auditory cortices, in addition to the common communication between bilateral auditory cortices in non-AP musicians.
3. As largely accepted [Levitin, 2004; Levitin and Rogers, 2005; Schulze et al., 2013], if the perceptual and

TABLE I. Mean and standard deviation of demographics

Variables	Non-AP ($n = 9$)		AP ($n = 8$)		t/z-statistic	P-value
	Mean	(Std.)	Mean	(Std.)		
Sex ratio (Women/all)	0.56	-	0.62	-	0.22	0.823
Age (years)	25.78	(5.19)	26.88	(2.95)	0.53	0.607
Handedness (LQ)	90.56	(11.54)	95	(9.26)	0.87	0.399
MET-melody hit rate (%)	82.26	(11.12)	91.11	(10.02)	1.71	0.107
$-\log_{10}$ FDT	2.41	(0.23)	2.73	(0.68)	−1.34	0.199
Ethnicity ratio (Asian/all)	0.00	-	0.38	-	2.91	0.004
Onset of musical training (year)	8.00	(2.96)	5.00	(1.51)	−2.88	0.012
Musical training duration (year)	16.9	(7.83)	23.00	(3.34)	2.04	0.059

Abbreviations: FDT, frequency discrimination threshold [Micheyl et al., 2006]; LQ, laterality coefficient, ranging from −100 (exclusively left-handed) to 100 (exclusively right-handed) [Oldfield, 1971]; MET, Musical Ear Test (Wallentin et al., 2010); Std., standard deviation.

associative processes of AP perception are localized in the temporal and frontal structures, respectively, integration of the two parts is crucial for the successful realization of AP [Elmer et al., 2015]. In particular, the ventral auditory pathway from PAC, via PP, to the VLPFC is expected to show greater RSFC in relation to the acuity of AP. From a previous study [Wengenroth et al., 2014], the left IFG showed greater BOLD activation in passive response to musical tones. Considering the dominance of the left hemisphere in language functions, the association of the pitch chroma representation with the verbal label is likely to be processed in the left hemisphere.

In addition, because the left PT and left dorsal pathway have been implicated in several previous studies on the neural correlates of AP [Keenan et al., 2001; Oechslin et al., 2009; Schlaug et al., 1995; Wilson et al., 2009], as detailed above, the possibility of AP-related RSFC via the dorsal pathway should not be ignored. Thus, we also analyzed the RSFC of the posterior part of STP (including PT) for a fair comparison between the ventral and dorsal pathways in terms of association with AP.

Importantly, a previous rs-fMRI study reported greater overall (network-wise) degree centrality (i.e., the average number of edges across all nodes) in AP than in non-AP musicians [Loui et al., 2012], suggesting a global reorganization of brain networks. In contrast, in the current study, we tested specific hypotheses on the role of particular anatomical regions that are expected to be involved in the AP-specific RSN, based on our previous study [Kim and Knösche, 2016].

MATERIALS AND METHODS

Participants and Behavioral Tests

We analyzed resting-state fMRI data from 17 musicians (8 AP musicians and 9 non-AP musicians) who also participated in the previous study on intracortical myelination [Kim and Knösche, 2016]. Assignment of groups (either with or without AP) was determined by a web-based AP test before recruitment (≥80% correct answers as AP). The local ethics committee approved the experimental protocol, and all participants submitted written informed consent prior to experiments. More detailed information can be found in the previous study [Kim and Knösche, 2016]. Demographics are matched, except for the year of onset for musical training and ethnicity (Table I). The Asian musicians were from China (2), Japan (2), and Korea (1) and the European musicians were from Germany (11) and Russia (1). To match musical aptitude, we used a behavioral test called "Musical Ear Test" [Wallentin et al., 2010]. To measure pitch discrimination precision, we used a psychoacoustic test based on the staircase method [Micheyl et al., 2006]. We did not find any significant group difference in most demographic and behavioral measures (min $P > 0.06$), except for ethnicity ($P = 0.004$) and musical training onset age ($P = 0.012$). The ethnicity mismatch is because Asian musicians are much more likely to possess AP than European musicians [Miyazaki et al., 2012], which strongly impedes the recruitment of balanced cohorts. However, GLM results obtained from only European musicians were very similar to those from all musicians combined (cross-correlation between T-statistic maps with and without Asian musicians were between 0.96 and 0.98; see Supporting Information online for details), suggesting that confounding due to ethnicity was reasonably controlled for.

Behavioral testing on AP performance was carried out in our previous work [Kim and Knösche, 2016]. We calculated a scaled index (between 0 and 1; chance level of 0.5) of the acuity of AP that is called AP score (APS), which showed significant group difference between APs and non-APs ($P < 10^{-8}$ for pure tones; $P < 10^{-7}$ for piano tones). Further details of the behavioral experiments can be found elsewhere [Kim and Knösche, 2016].

Image Acquisition

Echo-Planar imaging (EPI) and magnetization-prepared rapid gradient-echo (MPRAGE) were acquired using a 3-T

MR system Magnetom Prisma (Siemens, Erlangen, Germany) with a 32-chanel head coil system. Within 10 minutes, 420 volumes of multi-band 2-D EPI with the acceleration factor of 4 were obtained, while the participant lay still and was instructed not to fall asleep with eyes closed. The imaging parameters of EPI were: time of repetition = 1400 ms, time of echo = 30 ms, flip angle = 60 degrees, image matrix = 88 × 88 × 64, voxel size = 2.295 × 2.295 × 2.300 mm^3. T1-weighted images using MPRAGE were also taken using a protocol based on the ADNI sequence[1] at 1-mm isotropic resolution during the same session. To correct for nonlinear distortions in the EPI images due to the inhomogeneous susceptibility in the static field, field maps in the identical geometry of the EPI were also acquired [Jezzard and Balaban, 1995].

Image Processing

Anatomical and functional images were preprocessed using SPM12.[2] The blood oxygen level-dependent (BOLD) images were first corrected for the multiband slice timing, unwarped and realigned, and resampled at 2.3-mm isotropic resolution using a fourth degree B-spline. To minimize spurious correlation due to head movements [Power et al., 2012], we adopted the "anatomical CompCor" approach. The main idea of this approach is that the signal fluctuation from the white matter (WM) and cerebrospinal fluid (CSF) voxels would not be due to neuronal activities [Behzadi et al., 2007]. Based on the T1-weighted image, WM and CSF voxels are determined by tissue probability over 99% and formed nonneural BOLD time series. Using principal component analysis (PCA), 16 principle components were extracted from the nonneural time series and used as "CompCor regressors." In addition, we also used other regressors for nonneural fluctuation: six rigid-motion parameters (three translations and three rotations with respect to the first volume) and the lengths of temporal derivative of the translation and rotation. The effects of nonneural regressors (16 CompCor regressors and 8 motion parameters) were fitted by least square estimation, and regressed out from the BOLD time series. This residual time series was then temporally filtered by a band-pass-filter between 9 and 80 mHz (i.e., 0.009 and 0.08 Hz) [Satterthwaite et al., 2013] for the FC measure of cross-correlation.

Geometrically, the boundaries of the cerebral cortex are highly convoluted sheets, which are essentially 2-D manifolds embedded in 3-D space [Chung et al., 2003]. Importantly, topology has been suggested as a crucial organizational principle of the cerebral cortex in primate brains [van Essen and Zeki, 1978]. Before the advent of MRI scanning and computational neuroanatomy, neuroscientists desired a method to flatten the cerebral cortex onto a 2-D plane to investigate functional architecture of the cortex [van Essen and Maunsell, 1980], which later motivated the development of computational methods for "virtual flattening" [van Essen et al., 2001]. In this study, we used surface-based methods for analyzing functional connectivity of the cortex [Yeo et al., 2011]. While the surface-based analysis has the advantage that it respects the intrinsic geometry of the cortex [Chung et al., 2003], its validity is heavily dependent on the quality of additional image processing compared to volume-based analysis. Thus, we carefully optimized our processing pipeline with thorough visual inspection at each stage. The T1-weighted image was skull-stripped using the unified segmentation [Ashburner and Friston, 2005] in SPM12 and then fed into FreeSurfer version 5.3.0[3] to reconstruct the cortical surface. Inner and outer boundaries of the cortex were modeled by two surfaces (an outer surface called "pial surface" and an inner surface called "white matter surface") for each hemisphere. The transform matrix from the EPI space to the T1-weighted image space was estimated using a boundary-based registration (BBR) approach [Greve and Fischl, 2009]. Then, the residual time series was resampled at the middle depth of the cortex (i.e., halfway between the pial and white matter surfaces) after nonneural fluctuations had been regressed out. The resampling depth was chosen to avoid partial volume effects while maintaining a high signal-to-noise ratio of the BOLD signal [Yeo et al., 2011].

The surface-projected residual time series were nonlinearly registered onto a low-resolution template mesh called "fsaverage5" in FreeSurfer via spherical mapping based on the local curvature of the surfaces. The registered time series were then spatially smoothed using a 2-D Gaussian kernel with the full width at half-maximum (FWHM) of 10 mm to minimize the effect of imperfection in intra-/intersubject registration. The seed mask was taken from our previous study [Kim and Knösche, 2016]; a cluster showing a significant group difference (i.e., greater cortical myelin in AP musicians) in the right PP. The mean MNI coordinate was (48, −5, −11) mm and the area was 44 mm^2. The first principal component (PC1) was then extracted from the seed mask. FC measures (explained below) were computed between the PC1 and residual time series for the rest of cortex.

Functional Connectivity Analysis

We used two different FC measures for analysis: cross-correlation and cross-coherence. The main motivation for using these measures is to reliably capture both delay-specific and frequency-specific connectivity differences. Cross-coherence is most sensitive to functional connectivity specifically occurring in particular frequency bands. It therefore emphasizes resonance phenomena between distant oscillators. In contrast, cross-correlation does not distinguish between frequencies, but instead is sensitive to coupling occurring with particular delays. Hence, it

[1]http://adni.loni.usc.edu/methods/documents/mri-protocols/

[2]http://www.fil.ion.ucl.ac.uk/spm/software/spm12/

[3]http://freesurfer.net/

emphasizes connectivity supported by particular axonal pathways (e.g., direct vs. indirect or slow vs. fast fibers). See Supporting Information online for a more detailed explanation with a toy example.

While cross-correlation and cross-coherence have been extensively used in analyzing electrophysiology data [Ostojic et al., 2009], they are relatively uncommon measures in fMRI analysis. Thus, we will explain the definition and characteristics of the measures and introduce previous studies on cross-correlation and cross-coherence in the BOLD time series below.

Cross-correlation of two time series, i and j, with a time lag h is given by:

$$\rho_{ij}(h)=\frac{\mathrm{cov}_{ij}(t,t+h)}{\sqrt{\mathrm{var}_i(t)\mathrm{var}_j(t+h)}}, \quad (1)$$

where $\rho_{ij}(h)=\rho_{ji}(-h)$, which is restricted to the interval [–1, 1]. If the time lag h equals zero, the zero-lag cross-correlation $\rho_{ij}(0)$ is equivalent to Pearson's coefficient of correlation, which we also used for the analysis. We segmented the time-lag of interest (± 100 s) into nine bins with a 50% overlap (i.e., [–100, −60], [–80, −40], …, [60, 100] s) and averaged cross-correlation maps with a certain range of time-lags within each bin.

Cross-coherence of two time series, i and j, at a frequency λ is given by:

$$\mathrm{coh}_{ij}(\lambda)=|R_{ij}(\lambda)|^2=\frac{|f_{ij}(\lambda)|^2}{f_i(\lambda)f_j(\lambda)}, \quad (2)$$

where $R_{ij}(\lambda)$ is the complex valued coherency, $f_i(\lambda)$ is the spectral density function at frequency λ, and $f_{ij}(\lambda)$ is the cross-spectral density function. Squared, coherence is a positive (bounded [0, 1]) and symmetric function (i.e., $\mathrm{coh}_{ij}(\lambda)=\mathrm{coh}_{ij}(-\lambda)$). Given the sampling rate of 714 mHz (i.e., 1/1.4 s × 1000) and the duration of 574 s (i.e., 410 volumes × 1.4 s) of the current data, the observable frequency range is between 1.714 (one cycle over the session) and 375 mHz (Nyquist–Shannon sampling theorem). Thus, we constrained our analysis within the frequency of interest of [2, 100] mHz and segmented it into 10 frequency bins with 50% overlap (i.e., [2, 20], [10, 30], …, [90, 110] mHz). Note that the binning was arbitrary to explore frequency-dependent connectivity.

Recent studies demonstrated the reliability of frequency-dependent BOLD fluctuation at rest [Achard and Bullmore, 2007; Achard et al., 2006; Cordes et al., 2001; De Luca et al., 2006; Qian et al., 2015; Salvador et al., 2005a,b; Sasai et al., 2014; Sun et al., 2004]. Whereas biological implications of the frequency of FC based on BOLD measures are yet to be further revealed, fMRI and fNIRS studies showed an association between the frequency and direction of connectivity: a low frequency coherence (9–100 mHz) for interhemispheric FC and a high frequency coherence (40–100 mHz) for fronto-occipital FC [Sasai et al., 2011]. Because we hypothesized increased RSFC between bilateral ventral auditory pathways in the musicians with AP, we expected to observe higher coherence in a low frequency band between the homologous auditory cortices.

Statistical Inference

We tested the effect of AP and APS as:

$$FC=\beta_0+motion\beta_1+ethnicity\beta_2+X\beta_3+\epsilon \quad (3)$$

where FC is either cross-correlation or cross-coherence, *motion* is a maximal temporal derivative of the head motion [Power et al., 2015], *ethnicity* is a binary variable for being either Asian or European, X is either AP, which is a group index, or APS, which is a behavioral measure of the acuity of AP, and ε is the Gaussian error variable. Note that we tested the effect of APS over all musicians, in addition to the group difference, because it is known that AP is not strictly dichotomic but shows some gradation: Musicians with an intermediate level of AP are also known as "quasi-AP" [Miyazaki, 2004; Wilson et al., 2009].

Statistical inference on the correlation maps with multiple comparisons correction based on the random field theory (RFT) was done using SurfStat[4] [Worsley et al., 2009] in the MATLAB environment (version 8.2; Mathworks, Inc., Natick, MA, USA). RFT-corrected cluster-level P-values were further multiplied by 4 as additional Bonferroni correction for the number of tests (i.e., two contrasts and two hemispheres).

Because the cross-correlation and cross-coherence maps are positively dependent between adjacent time-lags and frequency bins, respectively, we additionally used the false discovery rate (FDR) for the multiple comparisons across time-lags and frequency bands [Genovese et al., 2002]: that is, finding a threshold for the RFT-corrected cluster-wise P-values that makes FDR <0.05, and then applying the P-value threshold over all lags/bins.

Correlation between Cortical Myelin and Resting-State Functional Connectivity

In our previous study [Kim and Knösche, 2016], we found a positive correlation between the APS and the cortical myelin content in the right PP. In the current study, we hypothesized a positive relationship between the APS and RSFC of the right PP to a number of cortical areas. Such a correlation may lead us to assume a positive relationship between the cortical myelin and the RSFC of the right PP. However, as proven by Langford and colleagues, a positive correlation is not *transitive* unless the correlation coefficient is sufficiently close to 1 [Langford et al., 2001]. That is, a positive correlation between X and Y and that between Y and Z does not necessarily mean a positive correlation between X and Z. Therefore, as a confirmatory inference, we directly tested the relationship between intracortical

[4]http://www.math.mcgill.ca/keith/surfstat/

TABLE II. Coordinates and area of ROIs of planum temporale

Atlas/study	Structure name	MNI-coordinate of centroid (mm)	Area (mm^2)
FS: Desikan-a2009s	Left planum temporale	−57, −41, 15	56.5
	Right planum temporale	59, −34, 15	51.6
FSL: Harvard-Oxford	Left medial planum temporale	−44, −34, 11	43.9
	Right medial planum temporale	41, −31, 15	43.6
Luders et al. (2004)	Anterior planum temporale and Heschl's sulcus	−53, −18, 0	64.8
Wengenroth et al. (2014)	Left posterior superior temporal gyrus	−60, −29, 5	66.0
	Left posterior superior temporal gyrus	63, −36, 18	54.4
Dohn et al. (2015)	Right planum temporale	61, −12, 9	63.0

Abbreviations: ROI, region-of-interest; FS, FreeSurfer; FSL, FMRI Software Library.

myelination (indexed by the longitudinal relaxation rate qR1) in the right PP and RSFC between the right PP and the rest of the cortex using a simple GLM without covariates as:

$$FC = \beta_0 + qR_1\beta_1 + \epsilon \quad (4)$$

Control Analyzes Seeding from the Planum Temporale

As mentioned earlier, we particularly focused on the right PP and the ventral auditory pathway in the current study. This choice was motivated by the results of our previous study [Kim and Knösche, 2016] on myelination, the sensitivity of PP to pitch chroma [Warren et al., 2003b], and the dual pathway hypothesis [Rauschecker, 2012]. However, a number of neuroimaging studies reported group differences in the posterior STG, particularly the left PT [Keenan et al., 2001; Schlaug et al., 1995; Wilson et al., 2009], and the dorsal pathway such as the left SLF [Oechslin et al., 2009]. Therefore, it would be fair to examine the RSFC of the dorsal pathway seeding from the PT to study the relative importance of the two pathways.

We adapted MNI-coordinates where the effect of AP was found in the previous studies [Dohn et al., 2015; Luders et al., 2004; Wengenroth et al., 2014]. Moreover, to consider anatomical studies that used gross anatomical measures (i.e., volume and area) of the PT [Keenan et al., 2001; Schlaug et al., 1995; Wilson et al., 2009], we adapted the center coordinates of the PTs from standard atlases (Harvard–Oxford cortical structural atlas provided in FMRI Software Library (FSL); "Desikan-a2009s" surface-based parcellation provided in FreeSurfer).

In total, eight ROIs in the left and right PTs were created in a similar size to the right PP seed ROI (i.e., 44 mm^2) as listed in Table II. We repeated the identical set of analyzes for the PT ROIs as for the right PP.

RESULTS

Effects of AP and APS in Cross-Correlation

From the right PP, strong correlations with the bilateral STPs were observed across all musicians ($n = 17$) as shown in Figure 2. For this connectivity, we found significantly greater correlation between the right PP and the right first transverse sulcus and lateral STG (FTS/LSTG-R) between AP and non-AP groups as given in Figure 3.

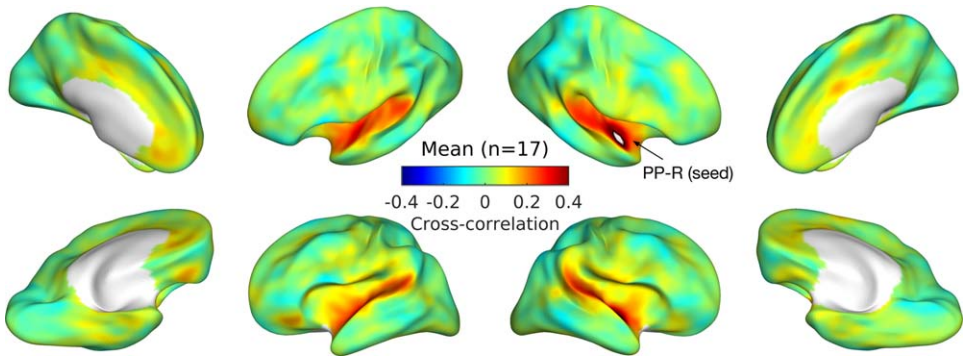

Figure 2.
Zero-lag cross-correlation between the right planum polare (PP-R; the white patch marked by the arrow) and the rest of the cortex are averaged across all individuals ($n = 17$). Correlations are projected onto minimally inflated cortical surfaces, which show major anatomical landmarks such as the Sylvian fissure. [Color figure can be viewed at wileyonlinelibrary.com]

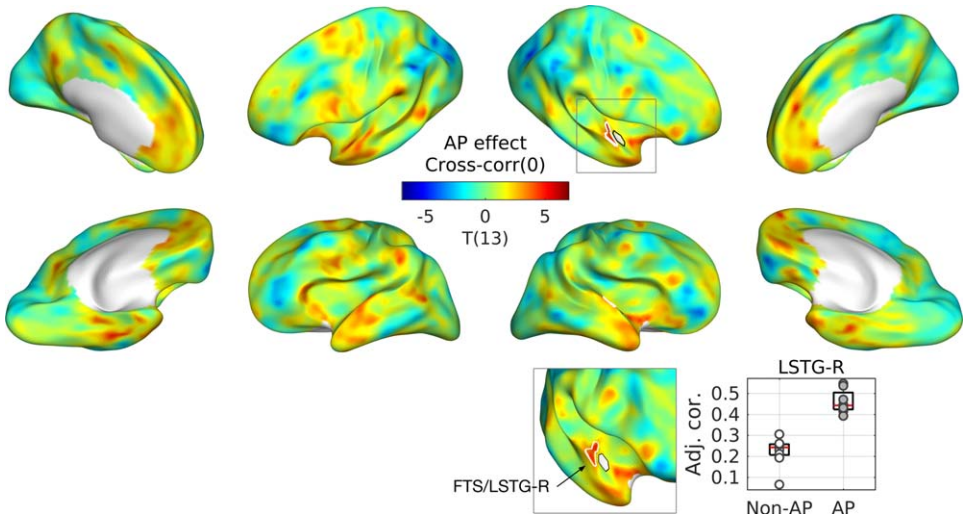

Figure 3.

Group difference between musicians with and without AP in zero-lag cross-correlation. T-statistic maps are projected onto semi-inflated cortical surfaces. Significant clusters are indicated by white contours. T-statistic maps are projected onto semi-inflated cortical surfaces. Significant clusters are indicated by white contours. In an inset (upper right), a zoomed view from a different angle is given to show the cluster in the medial part of the supratemporal plane more clearly. A boxplot with regression lines (lower right) is given for the peak of the cluster. An open circle represents a musician without AP, and a gray circle represents a musician with AP. Abbreviations: Adj. Cor., correlation coefficient adjusted for the nuisance variables of ethnicity and head motion; FTS, first transverse sulcus; LSTG, lateral superior temporal gyrus. [Color figure can be viewed at wileyonlinelibrary.com]

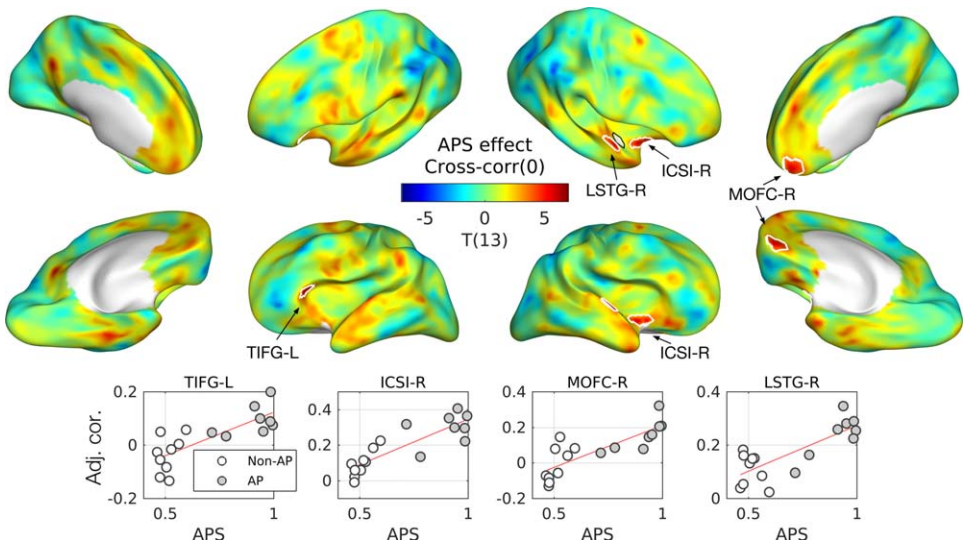

Figure 4.

Effects of absolute pitch score (APS) in zero-lag cross-correlation. T-statistic maps are projected onto semi-inflated cortical surfaces. Significant clusters are indicated by white contours. Below the T-maps, scatterplots with regression lines are given for the peak of each cluster. An open circle represents a musician without AP, and a gray circle represents a musician with AP. Abbreviations: ICSI-R, inferior segment of the circular sulcus of the right insula; LSTG-R, right lateral superior temporal gyrus; MOFC-R, right medial orbitofrontal cortex; TIFG-L, triangular part of the left inferior frontal gyrus. [Color figure can be viewed at wileyonlinelibrary.com]

TABLE III. Effects of absolute pitch (AP) and AP score (APS) in zero-lag correlation

Label	Effect size	Max T(13)	*P*-value[a]	Area (mm^2)	MNI-coord. (mm)	Full name of the structure[b]
Effect of AP						
FTS/LSTG-R	0.23	5.09	0.0270	60.1	46, −17, −3	Right first transverse sulcus; lateral aspect of the superior temporal gyrus
Effect of APS						
TIFG-L	0.66	5.38	0.0364	80.8	−42, 29, −2	Triangular part of the left inferior frontal gyrus
ICSI-R	0.88	5.83	0.0080	90.6	41, 3, −15	Inferior segment of the circular sulcus of the right insula
MOFC-R	0.91	5.60	0.0171	136.3	5, 54, −12	Right medial orbitofrontal cortex
LSTG-R	0.84	6.51	0.0241	39.0	62, 4, −5	Lateral aspect of the right superior temporal gyrus

[a]*P*-values are corrected for multiple comparisons.
[b]Identification of anatomical nomenclature is generally based on Destrieux Atlas (a2009s) and Desikan-Killiany-Tourville Atlas (DKTatlas40) in FreeSurfer.

For the APS, we found a positive effect in zero-lag cross-correlation in cortical regions that are adjacent to the right PP: the right lateral STG (LSTG-R) and the right inferior segment of the circular sulcus of the insula (ICSI-R). Moreover, we also found APS effects in frontal regions: the left triangular gyrus (TIFG-L) and the right medial orbitofrontal cortex (MOFC-R) as shown in Figure 3. Detailed statistics are given in Table III.

We did not find any effect of AP or APS in non-zero-lag cross-correlation over time-lags between ± 49 s ($P > 0.56$) or maps of absolute "best delay" ($P > 0.15$), which is the time-lag that maximizes cross-correlation (see Supporting Information online for averaged cross-correlation maps and best-delay maps).

Effects of AP and APS in Cross-Coherence

Averaged cross-coherence maps across all musicians for the first three frequency bins are given in Figure 5 (see Supporting Information online for all coherence maps). Compared to the zero-lag cross-correlation, the coherence maps are more widely distributed. Coherence values are generally higher in lower frequency bins (e.g., Figure 5,

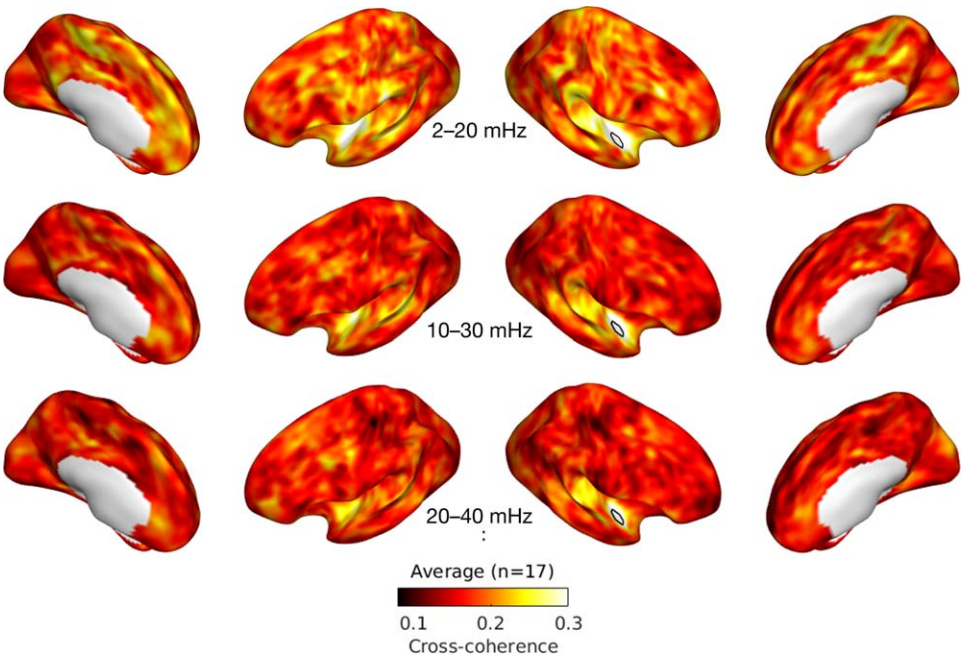

Figure 5.
First three averaged cross-coherence maps. Cross-coherence between the right planum polare (PP; marked by a white patch) and the rest of the cortex is averaged across all individuals ($n = 17$) for the first 3 frequency bins: 2–20 mHz (top), 10–30 mHz (middle), and 20–40 mHz (bottom). [Color figure can be viewed at wileyonlinelibrary.com]

top) compared to higher frequency bins (e.g., Figure 5, bottom).

We found significantly stronger cross-coherence in musicians with than without AP mostly at low frequency bins (i.e., < 40 mHz) as shown in Figure 6. In particular, we found the left planum polare and the left anterior STG in the frequency bin of 2–20 mHz, as well as bilateral superior temporal sulci (STSs) and the right middle temporal gyrus (MTG) in the frequency bin of 10–30 mHz. In addition, higher coherence in musicians with AP was found in medial frontal structures such as bilateral anterior cingulate cortices (ACCs) and the medial part of the superior frontal gyrus (SFG), as well as in other cortices including the inferior temporal gyrus (ITG), the cuneus (CNS), and the superior circular sulcus of insular cortex (SCSI).

Furthermore, we found a significant positive correlation between the cross-coherence of the right PP and APS in the right parietal-occipital sulcus (POS-R) and SFG-R as shown in Figure 7. The detailed statistics of the effects of AP and APS in cross-coherence are listed in Table IV.

Correlation between Cortical Myelin and Resting-State Functional Connectivity

We found a positive correlation between the AP/APS and RSFC of the right PP. Because we previously found positive a correlation between the AP/APS and cortical myelination (estimated by qR1) [Kim and Knösche, 2016], there might (but not necessarily) be a direct positive correlation between the myelination and RSFC of the right PP. To confirm this, we tested if the qR1 and RSFC of the right PP are also positively correlated (i.e., one-side T-test). We indeed found a positive effect of qR1 in the zero-lag cross-correlation between the right PP and the right first transverse sulcus (FTS) and LSTG as shown in Figure 8: $T(15) = 5.53$, beta = 15.8, $P = 0.026$, area = 70.8 mm^2, MNI-coordinate = (63, 0, −1) mm. Moreover, this suggests that the myeloarchitecture of a local circuit has a direct impact on its FC with adjacent regions, at least in this nonprimary auditory cortex.

Control Analyzes: RSFC of Planum Temporale

Finally, we tested the effects of AP and APS in the RSFC of the PT seeds to see whether the dorsal pathways also show similar effects to the ventral pathways. The locations of the ROIs of the PT [Dohn et al., 2015; Keenan et al., 2001; Luders et al., 2004; Schlaug et al., 1995; Wengenroth et al., 2014; Wilson et al., 2009] are shown in Figure 9. In all cases, we did not find any significant effect of AP or APS from the PT seeds (min $P = 0.094$). Minimal P-values from the control analyzes are tabulated in Table V.

DISCUSSION

In the current study, we investigated the effect of acuity of AP perception in the RSFC of a number of cortical areas that have previously been indicated in neuroimaging studies on AP, including the right PP that was recently found to be highly myelinated in AP listeners [Kim and Knösche, 2016]. In our data, only the right PP, but not the tested areas in the PT, exhibited significant relationships between AP and RSFC to other cortical areas. Moreover, we confirmed a direct relationship between myelination of the right PP and RSFC of that area to the adjacent cortex, suggesting functional implication of the cortical myelin in a nonprimary auditory cortex. As hypothesized, we found greater RSFC of the right PP with the adjacent ipsilateral auditory cortex (i.e., the right LSTG and the right STS/MTG) and the contralateral auditory cortices (i.e., the left PP/LSTG and the left STS) that are part of the ventral pathway, whereas the dorsal pathway (tested with multiple seeds of PT) did not show any such enhancement. Furthermore, we found additional evidence for the frontotemporal network integration and a close relationship between the auditory RSN and the DMN in AP listeners. In the following sections, we discuss the physiological plausibility and behavioral relevance of the current findings.

Resting State Functional Connectivity and Neural Interaction

It is commonly accepted that BOLD signals are closely related to neuronal activity, as, for example, supported by simultaneous measurement of local field potentials (LFPs) and BOLD in optogenetic rodents [Lee et al., 2010]. Consequently, RSFC is likely to be reflective of interactions between neural populations, mediated by neurovascular coupling, as supported by a line of studies [Achard and Bullmore, 2007; Achard et al., 2006; Britz et al., 2010; Cordes et al., 2001; De Luca et al., 2006; Ko et al., 2011; Qian et al., 2015; Salvador et al., 2005a,b; Sasai et al., 2014; Shmuel and Leopold, 2008; Sun et al., 2004].

As briefly mentioned earlier, RSFC studies demonstrated association between low-frequency BOLD signal and interhemispheric FC. In a seminal study on rs-fMRI [Salvador et al., 2005a], partial correlation and coherence in a relatively low fMRI frequency range (0.4–152 mHz) generally decayed over increasing Euclidian distance between the regions. However, the connectivity between homologous areas in different hemispheres remained strong despite their relatively long distances, which was absent in patients with acute brainstem ischemia [Salvador et al., 2005a]. The main source of bilateralism between homologous pairs remains unclear: it could be due to common inputs from subcortical structures or to interhemispheric coordination. The study mentioned above on patients with acute brainstem ischemia supports the former [Salvador et al., 2005a], whereas a case study on the RSFC of a split-brain supports the latter [Johnston et al., 2008]. In that case study [Johnston et al., 2008], the postoperative RSFC in a pediatric patient (6-year-old male) showed striking reduction, or absence, of bilateralism unlike the preoperative RSFC.

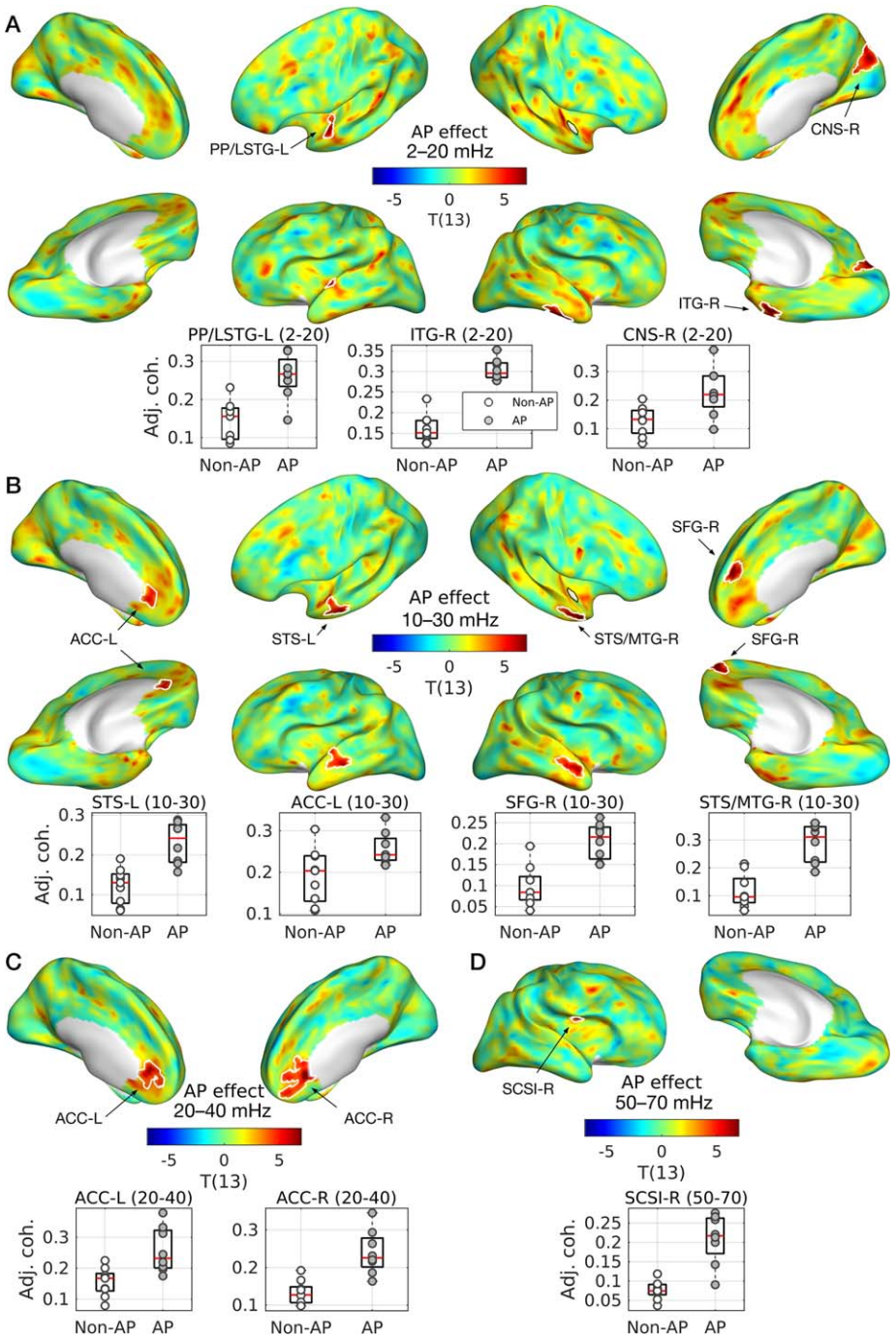

Figure 6.

Group differences between musicians with and without AP in cross-coherence. T-statistic maps are projected onto semi-inflated cortical surfaces for the frequency bin of (A) 2–20 mHz, (B) 10–30 mHz, (C) 20–40 mHz, and (D) 50–70 mHz. Significant clusters are indicated by white contours. Below the T-maps, boxplots with regression lines are given for the peak of each cluster. An open circle represents a musician without AP and a gray circle represents a musician with AP. Abbreviations: ACC-L/R, left/right anterior cingulate cortex; CNS-R, right cuneus; ITG-R, right inferior temporal gyrus; LSTG-L, lateral aspect of the left superior temporal gyrus; MTG-R, right middle temporal gyrus; SFG-R, right superior frontal gyrus; SCSI-R, superior segment of the circular sulcus of the right insula; STS-L, left superior temporal sulcus. [Color figure can be viewed at wileyonlinelibrary.com]

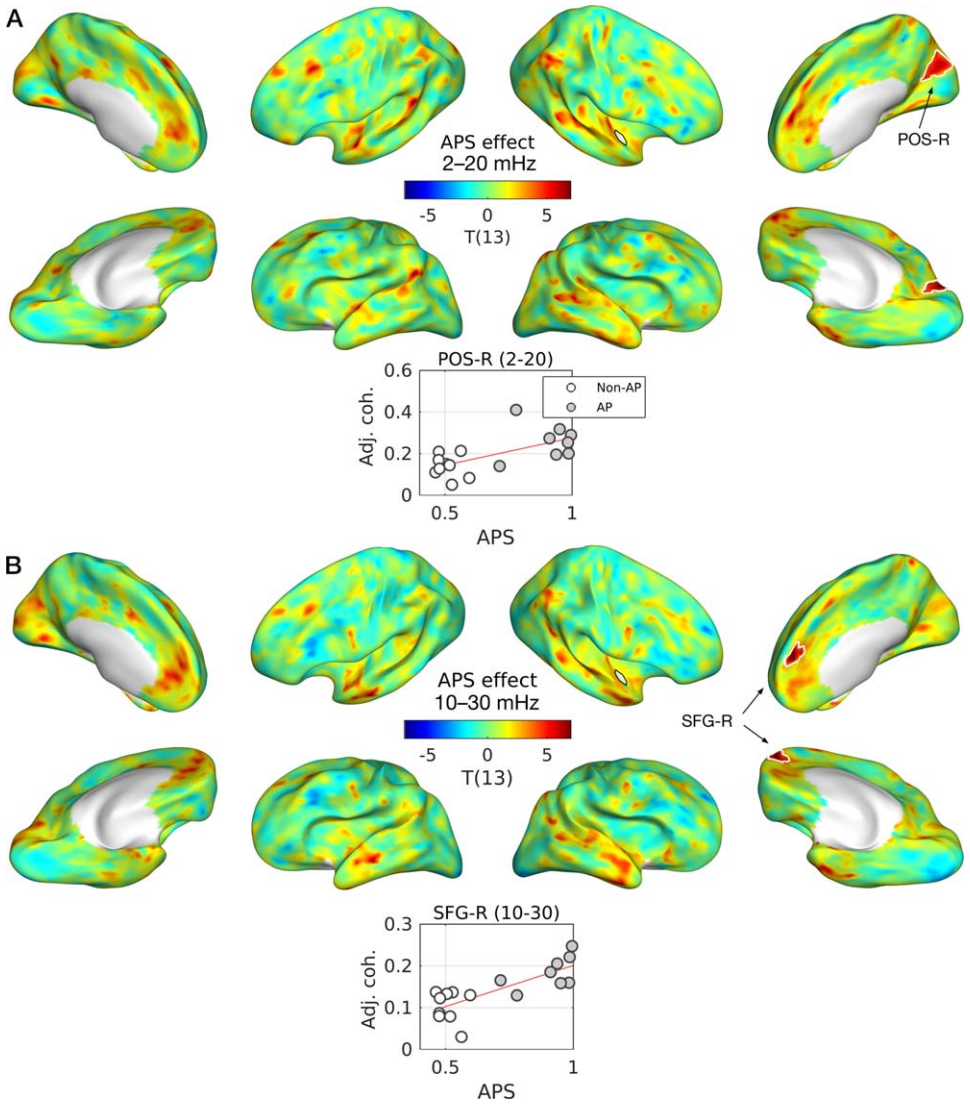

Figure 7.

Effects of absolute pitch score (APS) in cross-coherence. T-statistic maps are projected onto semi-inflated cortical surfaces. Significant clusters are indicated by white contours for the frequency bin of (A) 2–20 mHz and (B) 10–30 mHz. Below each T-map, boxplots with regression lines are given for the peak of each cluster. An open circle represents a musician without AP and a gray circle represents a musician with AP. Abbreviations: ACC-L/R, left/right anterior cingulate cortex; CNS-R, right cuneus; ITG-R, right inferior temporal gyrus; LSTG-L, lateral aspect of the left superior temporal gyrus; MTG-R, right middle temporal gyrus; SCSI-R, superior segment of the circular sulcus of the right insula; SFG-R, right superior frontal gyrus; STS-L, left superior temporal sulcus. [Color figure can be viewed at wileyonlinelibrary.com]

Regardless of its origin, the association between the low frequency and high coherence between homologous regions was further supported by a follow-up study [Salvador et al., 2005b]: In a relatively low frequency range (i.e., 4–152 mHz), mutual information between the homologous regions remained high over distance between ROIs, whereas such an effect was not found in a higher frequency range (i.e., 300–455 mHz). As revealed by fNIRS [Sasai et al., 2011], interhemispherical FC is also present in a low, wide frequency band (9–100 mHz), in addition to the fronto-occipital FC in a higher frequency range (40–100 mHz).

In the present study, as hypothesized, we also observed interhemispheric connectivity between the right PP and homologous or near-homologous cortical regions in the left hemisphere. As shown in Figure 5, the lowest

TABLE IV. Effects of absolute pitch (AP) and AP score (APS) in cross-coherence

Label	Freq. (mHz)	Effect size	Max T(13)	*P*-value[a]	Area (mm^2)	MNI-coord. (mm)	Full name of structure[b]
Effect of absolute pitch							
LSTG-L	2–20	0.31	7.72	0.0048	108.0	−61, 4, −6	Left lateral aspect of the superior temporal gyrus
ITG-R	2–20	0.31	14.40	0.0008	163.1	56, −15, −41	Right inferior temporal gyrus
CNS-R	2–20	0.34	6.84	0.0065	202.7	6, −78, 31	Right cuneus
STS-L	10–30	0.24	6.86	0.0016	161.6	−62, −8, −19	Left superior temporal sulcus
ACC-L	10–30	0.23	5.88	0.0108	148.6	−3, 37, −3	Left anterior part of the cingulate gyrus and sulcus
SFG-R	10–30	0.27	8.18	0.0027	142.6	7, 52, 25	Right superior frontal gyrus
MTG-R	10–30	0.31	6.60	0.0042	134.6	54, 8, −27	Right middle temporal gyrus
ACC-L	20–40	0.30	6.74	0.0034	271.4	−2, 42, 3	Left anterior part of the cingulate gyrus and sulcus
ACC-R	20–40	0.32	9.53	0.0002	437.2	3, 34, −2	Right anterior part of the cingulate gyrus and sulcus
SCSI-R	50–70	0.24	7.14	0.0112	62.3	40, −2, 15	Right superior segment of the circular sulcus of the insula
Effect of absolute pitch score							
POS-R	2–20	0.98	6.19	0.0036	222.5	6, −74, 27	Right parieto-occipital sulcus
SFG-R	10–30	0.79	10.25	0.0043	120.3	7, 52, 22	Right superior frontal gyrus

[a]*P*-values are corrected for multiple vertices using random field theory and multiple frequency bins using false discovery rate (FDR). The *P*-value threshold controlling FDR less than 0.05 was 0.0148 (AP) and 0.0043 (APS), respectively.
[b]Identification of anatomical nomenclature is generally based on the Destrieux Atlas (a2009s) and the Desikan-Killiany-Tourville Atlas (DKTatlas40) in FreeSurfer.

frequency bin (2–20 mHz) showed greater coherence over the whole cortex, especially between the homologous regions, in comparison to the relatively high frequency bins (e.g., 10–30, 20–40 mHz). This reconfirms and refines the picture of long-range interhemispheric connections being prominent in lower BOLD frequencies.

Ventral and Dorsal Auditory Pathways

As discussed earlier in the Introduction, we hypothesized higher FC via the ventral auditory pathway, unlike the dorsal auditory pathway, based on the implicated involvement of the ventral pathway in processing nonspatial categorical auditory information [Altmann et al., 2007; Barrett et al., 2005; Barrett and Hall, 2006; Hart et al., 2004] and the reported importance of pitch chroma in AP processing [Deutsch and Henthorn, 2004; Miyazaki, 1988, 2004; Takeuchi and Hulse, 1993]. In the current study, we discovered stronger RSFC of the right PP to several ventral auditory cortices in both hemispheres for musicians with AP bilaterally; these areas include the left PP/LSTG, the left STS, and the right STS extending to MTG. No such effect was found in the RSFC of any of 8 ROIs of PT for the dorsal pathway.

The STS is well known for specialized feature processing of complex but well-trained auditory stimuli such as the human voice [Belin et al., 2000, 2004], or, more generally, auditory information that aids identification of the sound source [Zatorre et al., 2004]. Given that pitch chroma could be viable information for object identification for AP listeners, the current finding of an AP-specific increase of RSFC supports our hypothesis on the involvement of the ventral pathway in the perceptual process of AP.

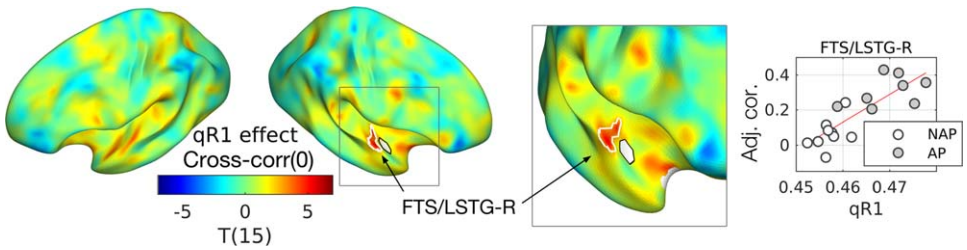

Figure 8.
Effect of cortical myelin (qR1) on cross-correlation. A significant cluster in the right first transverse sulcus and lateral superior temporal gyrus (FTS/LSTG-R) is marked with a scatterplot at the peak vertex. In an inset, a zoomed view from a different angle is also given to aid observation. Abbreviation: Adj. cor., adjusted zero-lag cross-correlation; qR1, quantitative longitudinal relaxation rate. [Color figure can be viewed at wileyonlinelibrary.com]

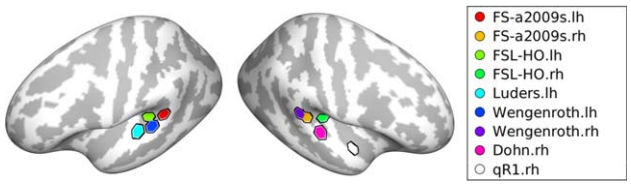

Figure 9.

Regions-of-interest (ROIs) in planum temporale (PT) used for control analysis. Atlases or reference studies are marked in colors. For reference, the ROI in the right planum polare used in the main analyzes is shown in white. Abbreviation: lh, left hemisphere; rh, right hemisphere. See Materials and Methods for references, on which the ROIs are based. [Color figure can be viewed at wileyonlinelibrary.com]

Moreover, the right PP showed stronger RSFC with the right FTS, which forms the anterior border of the HG [Schneider et al., 2005]. Given that cortical myelination after a critical period may prohibit neuroplasticity during typical neurodevelopment [McGee et al., 2005], pitch chroma relevant auditory information might be preserved in the right PP after the development of AP. Thus, the increased RSFC between the right PP and the ipsilateral lower-level auditory cortex (i.e., FTS) might reflect this chromatic categorization processing, although it remains largely unknown how the process is actually implemented in the interaction between the two regions, which could be template-matching, collective filtering, or other.

Previous neuroimaging studies on AP implicated the posterior part of the STP (i.e., PT) with an emphasis on the leftward laterality [Keenan et al., 2001; Schlaug et al., 1995] and its connection to the DLPFC [Elmer et al., 2015; Oechslin et al., 2009] via the left dorsal pathway. Conversely, we did not find effects of AP or APS in the RSFC for any of the tested 8 ROIs in the PT. Thus, our finding of the AP-specific RSFC in the bilateral ventral auditory pathway (and negative findings in the dorsal pathways) may appear to conflict with these previous studies. Although the discrepancy might be due to different samples and demographic controlling, we believe it is more likely to be related to different methodologies and analytic approaches used. Unlike the early volumetric studies [Keenan et al., 2001; Schlaug et al., 1995], whole-brain morphological studies [Bermudez et al., 2009; Dohn et al., 2015] reported significant differences in cortical thickness in both hemispheres. Moreover, Dohn and colleagues also found an AP-specific increase of FA in the right ventral pathway including the uncinate fasciculus (UF) and inferior longitudinal fasciculus (ILF), using whole-brain white matter analysis [Dohn et al., 2015].

Given the rapid processing of AP [Itoh et al., 2005; Miyazaki, 1988], linking chromatic categorization of a given tone with a lexical label and/or a motor program should be done very efficiently. Such high efficiency could be realized when specialized subprocesses are properly integrated. Based on our finding of increased FC between the right PP and bilateral ventral pathways (including the left PP and the bilateral STS), we suggest that the perceptual process of AP may be implemented via bilateral ventral pathways. The highly myelinated region in the right PP may perform initial processing of AP (presumably pitch chroma extraction), and the left IFG may be involved in verbal labeling, as suggested by Wengenroth and colleagues [Wengenroth et al., 2014].

However, the role of left PP remains unclear: It could either be involved in pitch chroma extraction in parallel with the right PP, or transfer the output of the right PP to the left IFG in a serial. These two possibilities cannot be differentiated from functional connectivity measures based on fMRI data. Effective connectivity measures based on noninvasive magneto-/electrophysiological measures with a high temporal precision (i.e., M/EEG) might provide an opportunity to quantitatively test it. A recent study on the interaction between auditory and motor cortices during an imitative vocalization task in AP listeners used dynamic causal modeling (DCM) of EEG data with ROI selection derived from fMRI data [Parkinson et al., 2014]. Such an

TABLE V. Coordinates and minimal *P*-values for the effects of AP and APS in RSFC of the planum temporale

Label	Structure name	Min P^a (cor.)		Min P^b (coh.)	
		AP	APS	AP	APS
FS-a2009s.lh	Left planum temporale	1.000	0.550	0.153	0.237
FS-a2009s.rh	Right planum temporale	0.367	0.201	0.094	0.298
FSL-HO.lh	Left medial planum temporale	0.257	1.000	0.152	0.122
FSL-HO.rh	Right medial planum temporale	0.368	0.208	0.144	0.229
Luders.lh	Anterior planum temporale and Heschl's sulcus	0.163	0.548	0.144	0.171
Wengenroth.lh	Left posterior superior temporal gyrus	1.000	1.000	0.177	0.320
Wengenroth.rh	Left posterior superior temporal gyrus	0.979	1.000	0.178	0.174
Dohn.rh	Right planum temporale	0.185	0.192	0.145	0.113

[a]P-values are corrected for multiple comparisons across vertices using random field theory (RTF).
[b]*P*-values are further adjusted for multiple comparisons across frequency bands using false discovery rate.
Abbreviations: aPT, anterior PT; BA, Brodmann area; cor., cross-correlation; coh., cross-coherence; mPT, medial PT; PT, planum temporale; pSTG, posterior superior temporal gyrus.

approach using multimodal data with different timescales could be useful to further elucidate the role of the left ventral pathway in AP processing.

Link to the Default-Mode Network

The DMN was initially suggested from the decrease of blood flow during language-related tasks compared to resting during PET experiments [Shulman et al., 1997] and has been further established by subsequent fMRI studies [Greicius et al., 2003; Smith et al., 2009]. Given that the notion of "default-mode" came from the deactivation, many studies related the DMN to internally generated processes, such as, for example, self-referential episodic memory, prospection, and theory of mind [Greicius and Menon, 2004; Spreng et al., 2009]. The auditory RSN usually shows anticorrelation with the DMN and positive correlation with the "salience network" (SN) [Menon, 2011], which directs attention to the sensory inputs. This anticorrelation between the DMN and SN seems to reflect "deactivation" during rest (i.e., negative contrast from the subtraction of "rest" condition from "stimulus" condition) in block-designed fMRI experiments [Greicius and Menon, 2004].

Interestingly, in the current study, the auditory RSN based on the right PP showed APS-related neural coupling to the medial frontal structures, that is, the ACCs and the medial SFG, which are known to be crucial nodes of the DMN [Greicius et al., 2003, 2009; Smith et al., 2009; Zald et al., 2014]. The frequency bands of the found coherence (10–30 mHz and 20–40 mHz) were also in accordance with one of the few multimodal BOLD imaging studies using simultaneous fMRI and fNIRS [Sasai et al., 2014] that reported a high degree centrality of the ACC in a low frequency band (10–30 mHz). Increased RSFC between the right PP and DMN network might be related to the spontaneous nature of AP-related processing that is even active during rest, which could result in unintentional recognition of AP [Miyazaki, 2004].

Insular and Other Cortices

We found stronger RSFC between the right PP and the inferior/superior segment of the circular sulcus of the insula. Auditory regions of the insula in human brains have been implicated from cytoarchitecture studies [Rivier and Clarke, 1997], microelectrode recording in patients [Remedios et al., 2009], and fMRI studies [Bamiou et al., 2003]. It has been previously shown that the anterior insula is involved in auditory object identification [Binder et al., 2004]. Additionally, dissection of the anterior insula in epileptic patients impaired verbal naming of familiar faces, but conceptual knowledge remained intact [Papagno et al., 2010], suggesting the implication of the insula in the verbal labeling process in AP recognition.

We also found higher RSFC in the right cuneus and anterior part of the right ITG. Although this may be somewhat unexpected, modulation in the visual system (i.e., cuneus) due to lexical-semantic priming in processing spoken language has been reported before [Kotz et al., 2002; Rämä et al., 2012]. Additionally, the anterior part of the ITG has been related to domain-general conceptual knowledge [Rice et al., 2015] and semantic networks with the stronger association in the left hemisphere [Cousins et al., 2016]. Taken together, AP processing might not be limited to only verbal labeling but also related to semantic representations, as postulated by Dohn and colleagues [Dohn et al., 2015].

Limitations

We note that the current study with rs-fMRI data, without task-based fMRI data, has an inherent limitation in terms of generalizability. That is to say, from the data at hand, we are unable to answer the question whether the detected functional connectivity pattern also remains similar during active cognitive processing. However, from a large-scale database, correspondence between the RSNs and functional networks during cognitive processes, or their subnetworks associated with "cognitive ontology," has been suggested [Smith et al., 2009; Yeo et al., 2015].

The mismatch in ethnicity still remains because the current datasets were acquired from the same participants as in our previous study [Kim and Knösche, 2016]. However, we have demonstrated that the effect size estimation is relatively accurate under the current experimental design by simulations in the previous article. Furthermore, the main findings in our previous and current studies were replicated with only the European musicians, clearly showing that they were not due to the confounding effect of ethnicity.

CONCLUSION

The right PP, which had been identified as being more heavily myelinated in AP musicians, was found to be part of an AP-related network of RSFC. Importantly, this network includes bilateral ventral auditory pathways (i.e., the bilateral PP and STS, and the left IFG), whereas the dorsal pathway did not show any association with AP ability. Moreover, the network also showed tight coupling between the right PP and crucial nodes of the DMN (i.e., bilateral ACC and the right medial SFG), which may reflect the spontaneity and automaticity of AP. The current study demonstrates the functional relevance of cortical myelin that is mediated by a rare variant of auditory perception.

ACKNOWLEDGMENTS

We thank Jae-Hyun Cho for valuable advice on functional connectivity measures. We also thank the anonymous reviewers and associate editor for constructive comments

that helped us to improve the manuscript substantially. This work was supported by the International Max-Planck Research School on Neuroscience of Communication (IMPRS NeuroCom).

REFERENCES

Achard S, Bullmore E (2007): Efficiency and cost of economical brain functional networks. PLoS Comput Biol 3:174–183.

Achard S, Salvador R, Whitcher B, Suckling J, Bullmore E (2006): A resilient, low-frequency, small-world human brain functional network with highly connected association cortical hubs. J. Neurosci 26:63–72.

Altmann CF, Bledowski C, Wibral M, Kaiser J (2007): Processing of location and pattern changes of natural sounds in the human auditory cortex. Neuroimage 35:1192–1200.

Arnott SR, Binns MA, Grady CL, Alain C (2004): Assessing the auditory dual-pathway model in humans. Neuroimage 22: 401–408.

Ashburner J, Friston KJ (2005): Unified segmentation. Neuroimage 26:839–851.

Baharloo S, Johnston PA, Service SK, Gitschier J, Freimer NB (1998): Absolute pitch: an approach for identification of genetic and nongenetic components. Am J Hum Genet 62:224–231.

Baharloo S, Service SK, Risch N, Gitschier J, Freimer NB (2000): Familial aggregation of absolute pitch. Am J Hum Genet 67: 755–758.

Bamiou D-E, Musiek FE, Luxon LM (2003): The insula (Island of Reil) and its role in auditory processing: Literature review. Brain Res Rev 42:143–154.

Barrett D, Hall D, Akeroyd M, Summerfield AQ (2005): The role of Heschl's gyrus (HG) in the analysis of pitch and spatial compactness, 12th Annual Meeting of the Cognitive Neuroscience Society. New York, NY, USA. 180 p.

Barrett DJ, Hall DA (2006): Response preferences for "what" and "where" in human non-primary auditory cortex. Neuroimage 32:968–977.

Behzadi Y, Restom K, Liau J, Liu TT (2007): A component based noise correction method (CompCor) for BOLD and perfusion based fMRI. Neuroimage 37:90–101.

Belin P, Fecteau S, Bedard C (2004): Thinking the voice: neural correlates of voice perception. Trends Cogn Sci 8:129–135.

Belin P, Zatorre RJ, Lafaille P, Ahad P, Pike B (2000): Voice-selective areas in human auditory cortex. Nature 403:309–312.

Bermudez P, Lerch JP, Evans AC, Zatorre RJ (2009): Neuroanatomical correlates of musicianship as revealed by cortical thickness and voxel-based morphometry. Cereb. Cortex 19: 1583–1596.

Bermudez P, Zatorre RJ (2005): Conditional associative memory for musical stimuli in nonmusicians: implications for absolute pitch. J Neurosci 25:7718–7723.

Binder JR, Liebenthal E, Possing ET, Medler DA, Ward BD (2004): Neural correlates of sensory and decision processes in auditory object identification. Nat Neurosci 7:295–301.

Bonzano L, Palmaro E, Teodorescu R, Fleysher L, Inglese M, Bove M (2015): Functional connectivity in the resting-state motor networks influences the kinematic processes during motor sequence learning. Eur J Neurosci 41:243–253.

Britz J, Van De Ville D, Michel CM (2010): BOLD correlates of EEG topography reveal rapid resting-state network dynamics. Neuroimage 52:1162–1170.

Cammoun L, Thiran JP, Griffa A, Meuli R, Hagmann P, Clarke S (2014): Intrahemispheric cortico-cortical connections of the human auditory cortex. Brain Struct Funct 220:3537–3553.

Chung MK, Worsley KJ, Robbins S, Paus T, Taylor J, Giedd JN, Rapoport JL, Evans AC (2003): Deformation-based surface morphometry applied to gray matter deformation. Neuroimage 18:198–213.

Cordes D, Haughton VM, Arfanakis K, Carew JD, Turski PA, Moritz CH, Quigley MA, Meyerand ME (2001): Frequencies contributing to functional connectivity in the cerebral cortex in "resting-state" data. AJNR Am J Neuroradiol 22:1326–1333.

Cousins KA, York C, Bauer L, Grossman M (2016): Cognitive and anatomic double dissociation in the representation of concrete and abstract words in semantic variant and behavioral variant frontotemporal degeneration. Neuropsychologia 84:244–251.

Damoiseaux JS, Rombouts SA, Barkhof F, Scheltens P, Stam CJ, Smith SM, Beckmann CF (2006): Consistent resting-state networks across healthy subjects. Proc Natl Acad Sci U S A 103: 13848–13853.

De Luca M, Beckmann CF, De Stefano N, Matthews PM, Smith SM (2006): fMRI resting state networks define distinct modes of long-distance interactions in the human brain. Neuroimage 29:1359–1367.

Deutsch D. 2013. The Psychology of Music. Amsterdam: Academic Press.

Deutsch D, Henthorn T (2004): Absolute pitch, speech, and tone language: Some experiments and a proposed framework. Music Percept 21:339–356.

Dohn A, Garza-Villarreal EA, Chakravarty MM, Hansen M, Lerch JP, Vuust P (2015): Gray- and white-matter anatomy of absolute pitch possessors. Cereb Cortex 25:1379–1388.

Elmer S, Rogenmoser L, Kuhnis J, Jancke L (2015): Bridging the gap between perceptual and cognitive perspectives on absolute pitch. J Neurosci 35:366–371.

Fauvel B, Groussard M, Chételat G, Fouquet M, Landeau B, Eustache F, Desgranges B, Platel H (2014): Morphological brain plasticity induced by musical expertise is accompanied by modulation of functional connectivity at rest. Neuroimage 90:179–188.

Genovese CR, Lazar NA, Nichols T (2002): Thresholding of statistical maps in functional neuroimaging using the false discovery rate. Neuroimage 15:870–878.

Geyer S, Weiss M, Reimann K, Lohmann G, Turner R (2011): Microstructural parcellation of the human cerebral cortex - from brodmann's post-mortem map to in vivo mapping with high-field magnetic resonance imaging. Front Hum Neurosci 5:19.

Greicius MD, Krasnow B, Reiss AL, Menon V (2003): Functional connectivity in the resting brain: A network analysis of the default mode hypothesis. Proc Natl Acad Sci U S A 100:253–258.

Greicius MD, Menon V (2004): Default-mode activity during a passive sensory task: uncoupled from deactivation but impacting activation. J Cogn Neurosci 16:1484–1492.

Greicius MD, Supekar K, Menon V, Dougherty RF (2009): Resting-state functional connectivity reflects structural connectivity in the default mode network. Cereb Cortex 19:72–78.

Greve DN, Fischl B (2009): Accurate and robust brain image alignment using boundary-based registration. Neuroimage 48:63–72.

Griffiths TD, Hall DA (2012): Mapping pitch representation in neural ensembles with fMRI. J Neurosci 32:13343–13347.

Griffiths TD, Warren JD (2002): The planum temporale as a computational hub. Trends Neurosci 25:348–353.

Hall DA, Plack CJ (2009): Pitch Processing Sites in the Human Auditory Brain. Cereb Cortex 19:576–585.

Hart HC, Palmer AR, Hall DA (2004): Different areas of human non-primary auditory cortex are activated by sounds with spatial and nonspatial properties. Hum Brain Mapp 21:178–190.

Itoh K, Suwazono S, Arao H, Miyazaki K, Nakada T (2005): Electrophysiological correlates of absolute pitch and relative pitch. Cereb Cortex 15:760–769.

Jezzard P, Balaban RS (1995): Correction for geometric distortion in echo planar images from B0 field variations. Magn Reson Med 34:65–73.

Johnston JM, Vaishnavi SN, Smyth MD, Zhang D, He BJ, Zempel JM, Shimony JS, Snyder AZ, Raichle ME (2008): Loss of resting interhemispheric functional connectivity after complete section of the corpus callosum. J Neurosci 28:6453–6458.

Kaas JH, Hackett TA (1999): 'What' and 'where' processing in auditory cortex. Nat Neurosci 2:1045–1047.

Keenan JP, Thangaraj V, Halpern AR, Schlaug G (2001): Absolute pitch and planum temporale. Neuroimage 14:1402–1408.

Kim S-G, Knösche TR (2016): Intracortical myelination in musicians with absolute pitch: quantitative morphometry using 7-T MRI. Hum Brain Mapp 37:3486–3501.

Ko AL, Darvas F, Poliakov A, Ojemann J, Sorensen LB (2011): Quasi-periodic fluctuations in default mode network electrophysiology. J Neurosci 31:11728–11732.

Kotz SA, Cappa SF, von Cramon DY, Friederici AD (2002): Modulation of the lexical–semantic network by auditory semantic priming: An event-related functional MRI study. Neuroimage 17:1761–1772.

Kusmierek P, Rauschecker JP (2009): Functional specialization of medial auditory belt cortex in the alert rhesus monkey. J Neurophysiol 102:1606–1622.

Langford E, Schwertman N, Owens M (2001): Is the property of being positively correlated transitive? Am Stat 55:322–325.

Lee JH, Durand R, Gradinaru V, Zhang F, Goshen I, Kim D-S, Fenno LE, Ramakrishnan C, Deisseroth K (2010): Global and local fMRI signals driven by neurons defined optogenetically by type and wiring. Nature 465:788–792.

Levitin DJ (2004): Absolute pitch: Self-reference and memory. Annee Psychol 104:103–120.

Levitin DJ, Rogers SE (2005): Absolute pitch: perception, coding, and controversies. Trends Cogn. Sci 9:26–33.

Loui P, Zamm A, Schlaug G (2012): Enhanced functional networks in absolute pitch. Neuroimage 63:632–640.

Luders E, Gaser C, Jancke L, Schlaug G (2004): A voxel-based approach to gray matter asymmetries. Neuroimage 22:656–664.

Luo C, Guo Z-w, Lai Y-x, Liao W, Liu Q, Kendrick KM, Yao D-z, Li H (2012): Musical training induces functional plasticity in perceptual and motor networks: insights from resting-state FMRI. PLoS One 7:e36568.

Marques JP, Gruetter R (2013): New developments and applications of the MP2RAGE sequence–focusing the contrast and high spatial resolution R1 mapping. PLoS One 8:e69294.

McGee AW, Yang Y, Fischer QS, Daw NW, Strittmatter SM (2005): Experience-driven plasticity of visual cortex limited by myelin and nogo receptor. Science 309:2222–2226.

Menon V (2011): Large-scale brain networks and psychopathology: a unifying triple network model. Trends Cogn. Sci 15:483–506.

Meyer M (1899): Is the memory of absolute pitch capable of development by training? Psychol Rev 6:514–516.

Micheyl C, Delhommeau K, Perrot X, Oxenham AJ (2006): Influence of musical and psychoacoustical training on pitch discrimination. Hear Res 219:36–47.

Miyazaki K (1988): Musical pitch identification by absolute pitch possessors. Percept Psychophys 44:501–512.

Miyazaki K (2004): How well do we understand absolute pitch?. Acoust Sci Technol 25:426–432.

Miyazaki K, Makomaska S, Rakowski A (2012): Prevalence of absolute pitch: A comparison between Japanese and Polish music students. J Acoust Soc Am 132:3484–3493.

Nieuwenhuys R (2013): The myeloarchitectonic studies on the human cerebral cortex of the Vogt-Vogt school, and their significance for the interpretation of functional neuroimaging data. Brain Struct Funct 218:303–352.

Oechslin MS, Imfeld A, Loenneker T, Meyer M, Jancke L (2009): The plasticity of the superior longitudinal fasciculus as a function of musical expertise: a diffusion tensor imaging study. Front Hum Neurosci 3:76.

Oldfield RC (1971): The assessment and analysis of handedness: the Edinburgh inventory. Neuropsychologia 9:97–113.

Ostojic S, Brunel N, Hakim V (2009): How connectivity, background activity, and synaptic properties shape the cross-correlation between spike trains. J Neurosci 29:10234.

Pandya DN, Hallett M, Mukherjee SK (1969): Intra-and interhemispheric connections of the neocortical auditory system in the rhesus monkey. Brain Res 14:49–65.

Papagno C, Miracapillo C, Casarotti A, Romero Lauro LJ, Castellano A, Falini A, Casaceli G, Fava E, Bello L (2010): What is the role of the uncinate fasciculus? Surgical removal and proper name retrieval. Brain 134:405–414.

Parkinson AL, Behroozmand R, Ibrahim N, Korzyukov O, Larson CR, Robin DA (2014): Effective connectivity associated with auditory error detection in musicians with absolute pitch. Front Neurosci 8:1–9.

Power JD, Barnes KA, Snyder AZ, Schlaggar BL, Petersen SE (2012): Spurious but systematic correlations in functional connectivity MRI networks arise from subject motion. Neuroimage 59:2142–2154.

Power JD, Schlaggar BL, Petersen SE (2015): Recent progress and outstanding issues in motion correction in resting state fMRI. Neuroimage 105:536–551.

Qian L, Zhang Y, Zheng L, Shang Y, Gao JH, Liu Y (2015): Frequency dependent topological patterns of resting-state brain networks. PLoS One 10:e0124681.

Rämä P, Relander-Syrjänen K, Carlson S, Salonen O, Kujala T (2012): Attention and semantic processing during speech: An fMRI study. Brain Lang 122:114–119.

Rauschecker JP (2012): Ventral and dorsal streams in the evolution of speech and language. Front Evol Neurosci 4:7.

Rauschecker JP (2015): Auditory and visual cortex of primates: a comparison of two sensory systems. Eur J Neurosci 41:579–585.

Rauschecker JP, Tian B (2000): Mechanisms and streams for processing of "what" and "where" in auditory cortex. Proc Natl Acad Sci U S A 97:11800–11806.

Remedios R, Logothetis NK, Kayser C (2009): An auditory region in the primate insular cortex responding preferentially to vocal communication sounds. J Neurosci 29:1034–1045.

Rice GE, Ralph MAL, Hoffman P (2015): The roles of left versus right anterior temporal lobes in conceptual knowledge: an ALE meta-analysis of 97 functional neuroimaging studies. Cereb Cortex:bhv024.

Rivier F, Clarke S (1997): Cytochrome Oxidase, Acetylcholinesterase, and NADPH-Diaphorase Staining in Human Supratemporal and Insular Cortex: Evidence for Multiple Auditory Areas. Neuroimage 6:288–304.

Salvador R, Suckling J, Coleman MR, Pickard JD, Menon D, Bullmore E (2005a): Neurophysiological architecture of

functional magnetic resonance images of human brain. Cereb Cortex 15:1332–1342.
Salvador R, Suckling J, Schwarzbauer C, Bullmore E (2005b): Undirected graphs of frequency-dependent functional connectivity in whole brain networks. Philos Trans R Soc Lond B Biol Sci 360:937–946.
Sasai S, Homae F, Watanabe H, Sasaki AT, Tanabe HC, Sadato N, Taga G (2014): Frequency-specific network topologies in the resting human brain. Front Hum Neurosci 8:1022.
Sasai S, Homae F, Watanabe H, Taga G (2011): Frequency-specific functional connectivity in the brain during resting state revealed by NIRS. Neuroimage 56:252–257.
Satterthwaite TD, Elliott MA, Gerraty RT, Ruparel K, Loughead J, Calkins ME, Eickhoff SB, Hakonarson H, Gur RC, Gur RE and others (2013): An improved framework for confound regression and filtering for control of motion artifact in the preprocessing of resting-state functional connectivity data. Neuroimage 64:240–256.
Schlaug G, Jancke L, Huang YX, Steinmetz H (1995): In-Vivo evidence of structural brain asymmetry in musicians. Science 267: 699–701.
Schneider P, Sluming V, Roberts N, Scherg M, Goebel R, Specht HJ, Dosch HG, Bleeck S, Stippich C, Rupp A (2005): Structural and functional asymmetry of lateral Heschl's gyrus reflects pitch perception preference. Nat Neurosci 8:1241–1247.
Schulze K, Mueller K, Koelsch S (2013): Auditory stroop and absolute pitch: an fMRI study. HumBrain Mapp 34:1579–1590.
Shirer WR, Ryali S, Rykhlevskaia E, Menon V, Greicius MD (2012): Decoding subject-driven cognitive states with whole-brain connectivity patterns. Cereb Cortex 22:158–165.
Shmuel A, Leopold DA (2008): Neuronal correlates of spontaneous fluctuations in fMRI signals in monkey visual cortex: implications for functional connectivity at rest. Hum Brain Mapp 29:751–761.
Shulman GL, Fiez JA, Corbetta M, Buckner RL, Miezin FM, Raichle ME, Petersen SE (1997): Common blood flow changes across visual tasks: II. Decreases in cerebral cortex. J Cogn Neurosci 9:648–663.
Siegel JA (1974): Sensory and verbal coding strategies in subjects with absolute pitch. J Exp Psychol 103:37–44.
Smith SM, Beckmann CF, Andersson J, Auerbach EJ, Bijsterbosch J, Douaud G, Duff E, Feinberg DA, Griffanti L, Harms MP and others (2013): Resting-state fMRI in the Human Connectome Project. Neuroimage 80:144–168.
Smith SM, Fox PT, Miller KL, Glahn DC, Fox PM, Mackay CE, Filippini N, Watkins KE, Toro R, Laird ARothers (2009): Correspondence of the brain's functional architecture during activation and rest. Proc Natl Acad Sci U S A 106:13040–13045.
Smith SM, Miller KL, Moeller S, Xu J, Auerbach EJ, Woolrich MW, Beckmann CF, Jenkinson M, Andersson J, Glasser MF and others (2012): Temporally-independent functional modes of spontaneous brain activity. Proc Natl Acad Sci U S A 109: 3131–3136.
Spreng RN, Mar RA, Kim AS (2009): The common neural basis of autobiographical memory, prospection, navigation, theory of mind, and the default mode: a quantitative meta-analysis. J Cogn Neurosci 21:489–510.
Sun FT, Miller LM, D'Esposito M (2004): Measuring interregional functional connectivity using coherence and partial coherence analyses of fMRI data. Neuroimage 21:647–658.
Takeuchi AH, Hulse SH (1993): Absolute Pitch. Psychol Bull 113: 345–361.
Tian B, Reser D, Durham A, Kustov A, Rauschecker JP (2001): Functional specialization in rhesus monkey auditory cortex. Science 292:290–293.
van Essen DC, Drury HA, Dickson J, Harwell J, Hanlon D, Anderson CH (2001): An integrated software suite for surface-based analyses of cerebral cortex. J Am Med Inform Assoc 8:443–459.
van Essen DC, Maunsell JHR (1980): Two-dimensional maps of the cerebral cortex. J Comp Neurol 191:255–281.
Van Essen DC, Ugurbil K, Auerbach E, Barch D, Behrens T, Bucholz R, Chang A, Chen L, Corbetta M, Curtiss SW (2012): The Human Connectome Project: a data acquisition perspective. Neuroimage 62:2222–2231.
van Essen DC, Zeki SM (1978): The topographic organization of rhesus monkey prestriate cortex. J Physiol 277:193–226.
Wallentin M, Nielsen AH, Friis-Olivarius M, Vuust C, Vuust P (2010): The Musical Ear Test, a new reliable test for measuring musical competence (vol 20, p 188, 2010). Learning and Individual Differences 20: 705 p.
Warren JD, Griffiths TD (2003): Distinct mechanisms for processing spatial sequences and pitch sequences in the human auditory brain. J Neurosci 23:5799–5804.
Warren JD, Uppenkamp S, Patterson RD, Griffiths TD (2003a): Analyzing pitch chroma and pitch height in the human brain. Annual N Y Acad Sci 999:212–214.
Warren JD, Uppenkamp S, Patterson RD, Griffiths TD (2003b): Separating pitch chroma and pitch height in the human brain. Proc Natl Acad Sci U S A 100:10038–10042.
Wengenroth M, Blatow M, Heinecke A, Reinhardt J, Stippich C, Hofmann E, Schneider P (2014): Increased volume and function of right auditory cortex as a marker for absolute pitch. Cereb Cortex 24:1127–1137.
Wilson SJ, Lusher D, Wan CY, Dudgeon P, Reutens DC (2009): The neurocognitive components of pitch processing: insights from absolute pitch. Cereb Cortex 19:724–732.
Worsley KJ, Taylor JE, Carbonell F, Chung M, Duerden E, Bernhardt B, Lyttelton O, Boucher M, Evans AC (2009): SurfStat: A Matlab Toolbox for the Statistical Analysis of Univariate and Multivariate Surface and Volumetric Data Using Linear Mixed Effects Models and Random Field Theory, 15th Annual Meeting of Organization for Human Brain Mapping. San Francisco, USA. p S102.
Yeo BT, Krienen FM, Sepulcre J, Sabuncu MR, Lashkari D, Hollinshead M, Roffman JL, Smoller JW, Zollei L, Polimeni JR and others (2011): The organization of the human cerebral cortex estimated by intrinsic functional connectivity. J. Neurophysiol 106:1125–1165.
Yeo BT, Krienen FM, Eickhoff SB, Yaakub SN, Fox PT, Buckner RL, Asplund CL, Chee MW (2015): Functional specialization and flexibility in human association cortex. Cereb Cortex 25:3654–3672.
Zald DH, McHugo M, Ray KL, Glahn DC, Eickhoff SB, Laird AR (2014): Meta-analytic connectivity modeling reveals differential functional connectivity of the medial and lateral orbitofrontal cortex. Cereb Cortex 24:232–248.
Zatorre RJ (2003): Absolute pitch: a model for understanding the influence of genes and development on neural and cognitive function. Nat Neurosci 6:692–695.
Zatorre RJ, Bouffard M, Belin P (2004): Sensitivity to auditory object features in human temporal neocortex. J Neurosci 24:3637–3642.
Zatorre RJ, Perry DW, Beckett CA, Westbury CF, Evans AC (1998): Functional anatomy of musical processing in listeners with absolute pitch and relative pitch. Proc Natl Acad Sci U S A 95:3172–3177.

Supporting Information

Title: Resting state functional connectivity of the ventral auditory pathway in musicians with absolute pitch

Authors: Seung-Goo Kim, Thomas R. Knösche

Affiliation: Research Group for MEG and EEG — Cortical Networks and Cognitive Functions Max Planck Institute for Human Cognitive and Brain Sciences, Leipzig, Germany

Corresponding author: Seung-Goo Kim
Postal address: Stephanstraße 1A, 04103 Leipzig, Germany
Phone: +49 341 9940 2618
Facsimile: +49 341 9940 2624
Email: sol@snu.ac.kr

Cross-correlation vs. cross-coherence

Zero-lag cross-correlation quantifies the linear relationship between two time series without time lag. Due to its simplicity, most of the resting-state functional magnetic resonance imaging (rs-fMRI) literature used this measure for functional connectivity (FC). However, cross-correlation and cross-coherence can describe temporal and spectral aspects of coupling of two time series. For a toy example, consider a pair of time series y_1 and y_2 consisting of three components as:

$$y_i = \sum_j \sin\left(w_i f_j \phi_i 2\pi\right),$$

where w is weight, f is frequency, **φ** is phase. The time series y_i is a mixture of the three components. To avoid overlaps between components, frequencies were assigned with prime numbers (i.e., f = 5, 13, or 23 Hz).

Two time series y_1 and y_2 were identical except the second component. By shifting the phase of the second component of the time series y_2, we can systematically change frequency-dependent coupling across two time series. Thus, the phases were varied as **φ** = 0, π/4, π/2, 3π/4, or π. Furthermore, to illustrate the difference between the cross-correlation and cross-coherence, we changed the weight of the second component to 0.5 or 1.5.

In Figure S10, each set of three panels shows waveforms of time series y_1 (red) and y_2 (blue) in the left column, a cross-correlogram in the middle column, and a cross-coherogram in the right column. Zero-lag correlation ("xcor(0)") is noted at the top of the cross-correlogram and cross-coherence for the second component ("xcoh(13)") is noted at the top of the cross-coherogram.

As the phase difference increases, both the zero-lag correlation and the cross-coherence at the second component's frequency (i.e., 13 Hz) decrease. But, it is notable that the decrease rate of the zero-lag correlation is slower than that of the cross-coherence when the weight of the frequency of interest is smaller than other components (Figure S10, A) and vice versa (Figure S10, B). That is, depending on the weight of a specific component that correlates with a regressor of interest, for instance AP group index, we may find a group difference only in the cross-correlation (when the weight is greater) or only in the cross-coherence (when the weight is smaller).

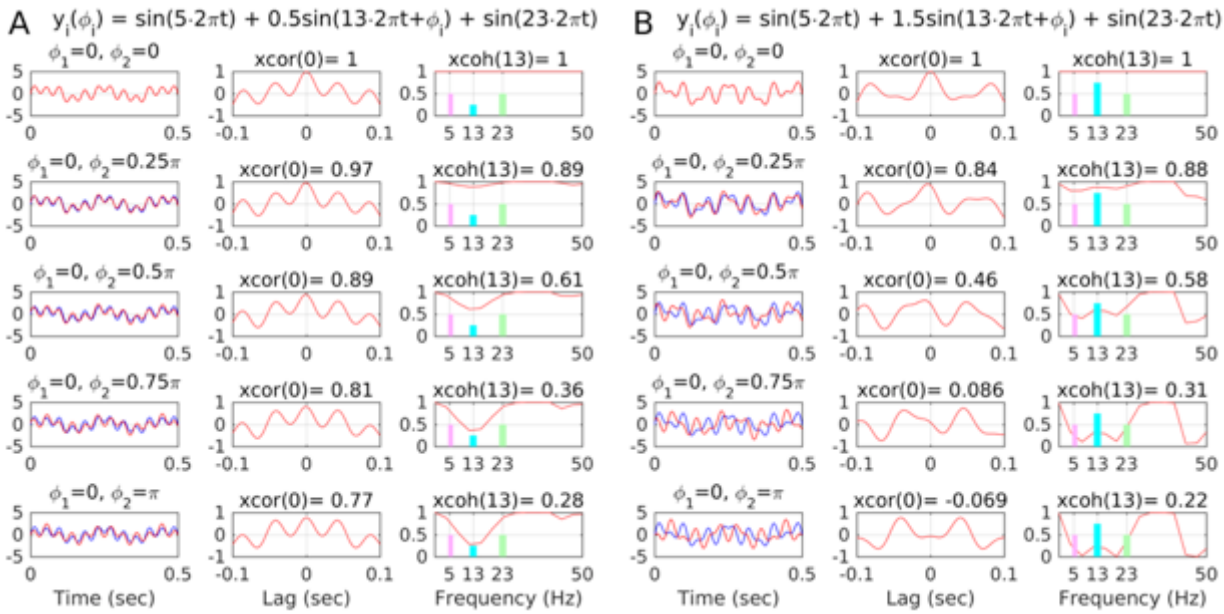

Figure S10. Toy examples on discrepancy between cross-correlation and cross-coherence. In all cases, the reference time series is created with constant phase of zero. For each panel, the weight of the second component (i.e., 13 Hz) is 0.5 (A) and 1.5 (B), respectively. For each row, the phase difference of the second component was 0 to π, and each column within a panel shows two time series (left column), cross-correlation (middle column), and cross-coherence (right column). Zero-lag correlation is noted above the plot for cross-correlation, whereas cross-coherence at the frequency of interest is noted above the plot for cross-coherence. The frequencies of 3 components are marked in the cross-coherence plot by vertical lines (magenta = 5 Hz, cyan = 13 Hz, green = 23 Hz). Abbreviations: xcor, cross-correlation; xcoh, cross-coherence.

Cross-correlation maps

We computed cross-correlation between the time series of the right planum polare (PP) as a seed region and the rest of the cortex over various time-lags between ± 100 s as shown in Figure S11. The magnitude of cross-correlation averaged across wide interval (40 s) was smaller (group averaged correlation between -0.07 and 0.08) compared to the zero-lag cross-correlation (between -0.11 and 0.98). Positive correlations in bilateral superior temporal planes (STPs) and the ventromedial prefrontal cortex (vmPFC), and anterior cingulate cortex (ACC) were shown around the zero-lag, whereas negative correlations in the STPs,

vmPFC, and ACC were found in longer lags. The cross-correlation maps were temporally symmetric in general but also showed asymmetry. For instance, the right frontal pole (marked by arrows) showed a positive correlation in negative lags (e.g., -40–0 s) but negative correlation at positive lag (e.g., 0–40 s) unlike STPs that showed a negative correlation in both positive and negative time-lags symmetrically.

Best delay is given a time-lag that maximizes cross-correlation. As already seen in cross-correlation maps, group-averaged best-delay maps (Figure S12) showed temporal asymmetry, for example, the right frontal pole (marked by a black arrow) showed maximal cross-correlation in negative lag, whereas the right superior frontal gyrus (marked by a white arrow) showed maximal correlation in positive lags. Bilateral STPs showed highest correlation in short time-lags and is clearly noticeable from the absolute value of best-delay maps (Figure S13). No effect of AP or APS was found from the non-zero cross-correlation maps or best-delay maps.

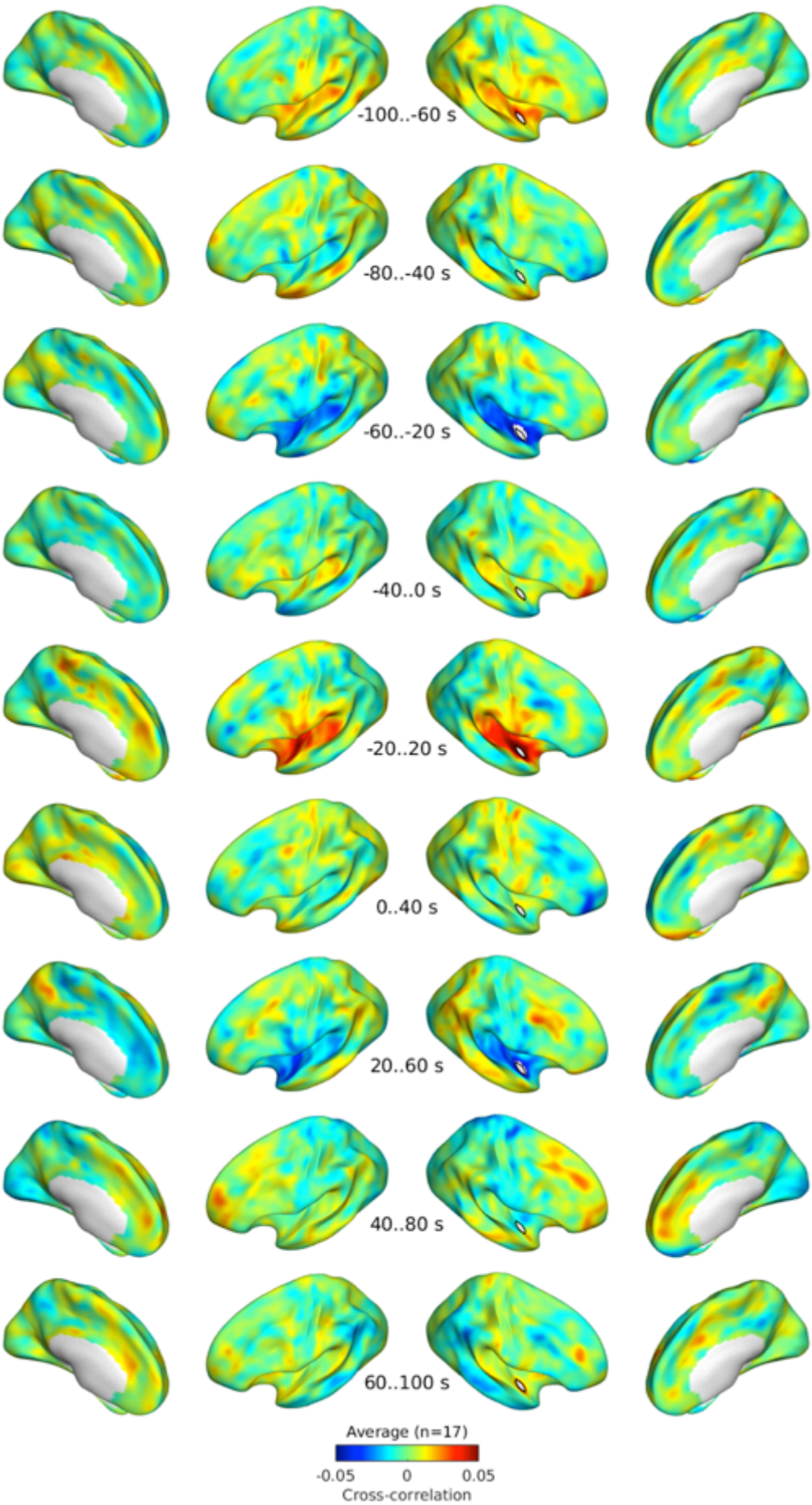
-100..-60 s
-80..-40 s
-60..-20 s
-40..0 s
-20..20 s
0..40 s
20..60 s
40..80 s
60..100 s
Average (n=17)
-0.05
0
0.05
Cross-correlation

Figure S11. Averaged (n = 17) cross-correlation over various time-lag between ± 100 s projected onto semi-inflated cortical surfaces from negative lag (top) to positive lag (bottom).

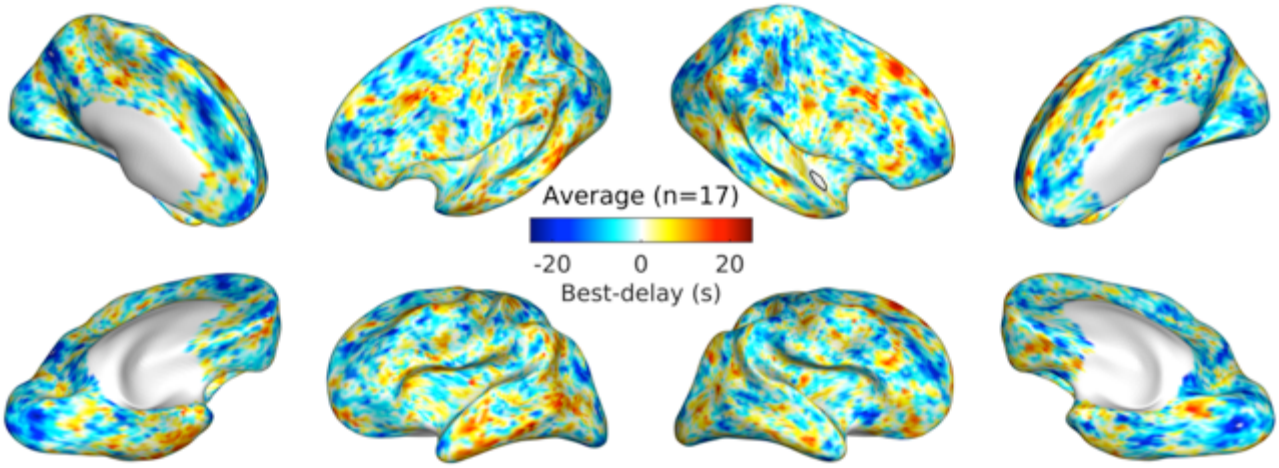

Figure S12. Best delay averaged over all subjects (n = 17) mapped on semi-inflated cortical surfaces.

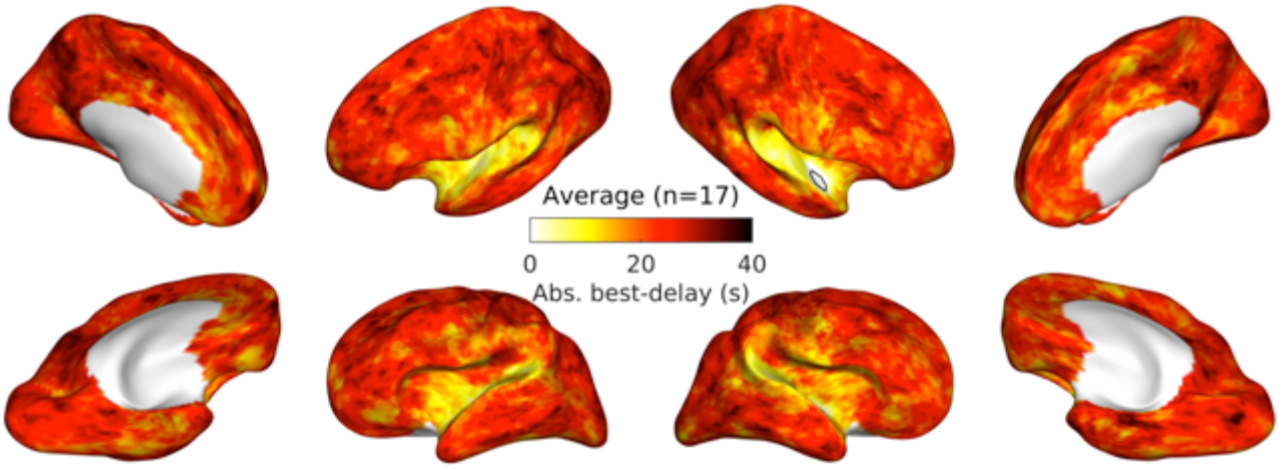

Figure S13. Absolute best delay averaged over all subjects (n = 17) mapped on semi-inflated cortical surfaces.

Cross-coherence maps

Averaged cross-coherence maps across all musicians for all the frequency bins are given in Figure S14. For a 50% overlap between adjacent frequency bins, the cross-coherence maps were similar but consistently showed high coherence on bilateral STPs and gradually smaller overall magnitudes in higher than lower frequency bins.

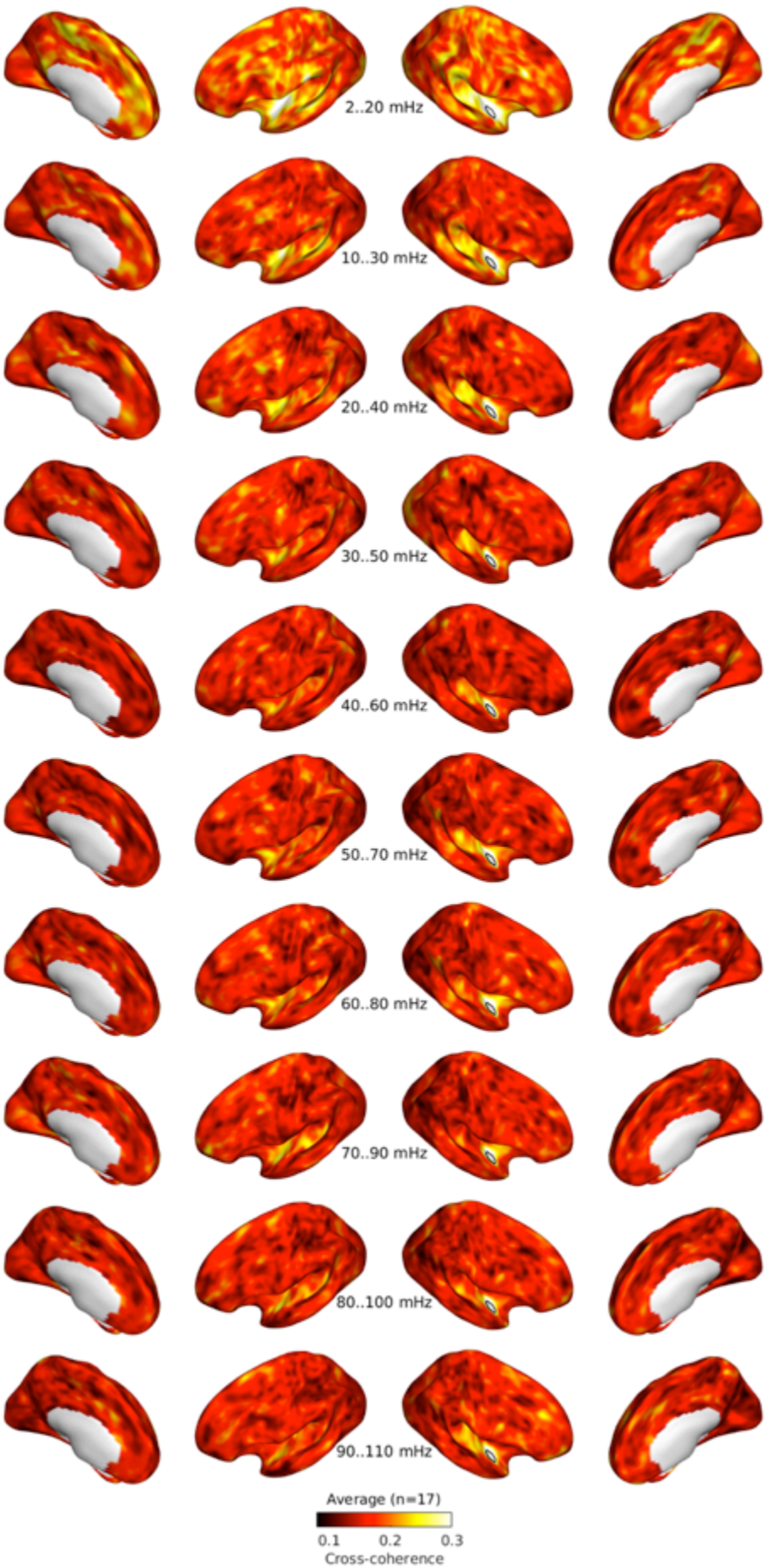
2..20 mHz
10..30 mHz
20..40 mHz
30..50 mHz
40..60 mHz
50..70 mHz
60..80 mHz
70..90 mHz
80..100 mHz
90..110 mHz
Average (n=17)
0.1
0.2
0.3
Cross-coherence

Figure S14. Averaged (n = 17) cross-coherence over multiple frequency bins between 2 and 110 mHz.

Replication only with European musicians

Because the current dataset includes ethnic diversity, its generalization might be limited. To demonstrate that the present findings are not due to the confounding effect of ethnicity, we tested GLMs again only with European but without Asian musicians for RSFC measures that showed significant effects in the main text (i.e., zero-lag cross-correlation and cross-coherence).

With European musicians only, we did not find a significant group difference (min p = 0.195) but found significant effect of APS in zero-lag cross-correlation in the right anterior insula (ICSI-R) and left inferior frontal gyrus (TIFG-L) as in Figure S15.

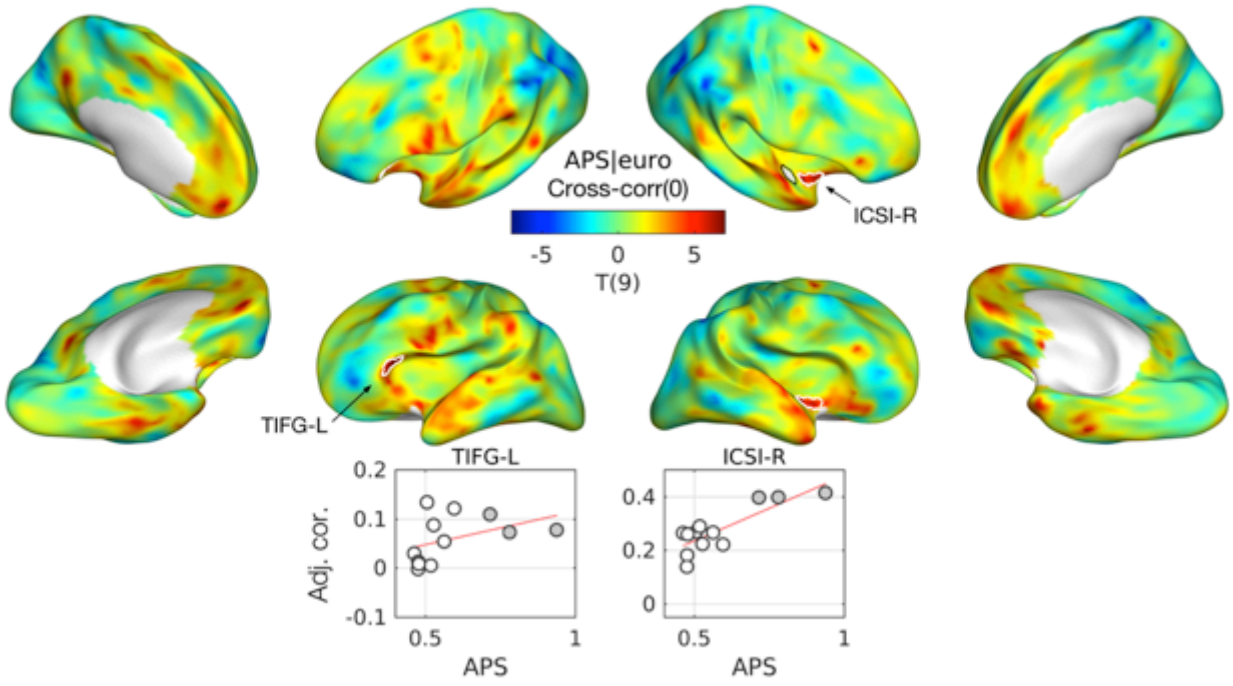

Figure S15. Effect of APS in zero-lag cross-correlation only with European musicians. T-statistic maps are projected onto semi-inflated cortical surfaces. Significant clusters are indicated by white contours. Below the T-maps, scatterplots with regression lines are given for the peak of each cluster. An open circle represents a musician without AP and a gray circle represents a musician with AP. Abbreviations: TIFG-L, triangular part of the left inferior frontal gyrus; ICSI-R, inferior segment of the circular sulcus of the right insula.

We also found a significant effect of AP in cross-coherence between 2 and 40 mHz but found no effect of APS in coherence as in Figure S16. As with the GLM analyses in the main text, the adjacent auditory

cortex (FTS/LSTG-R), the contralateral homologous auditory cortex (PP/LSTG-L), ventral auditory cortex (STS-L), and anterior cingulate cortex (ACC-L) were found to be different between the musicians with and without AP. Additionally, the inferior temporal structure (ITG-R) was found to be different between groups as in the analysis with all musicians.

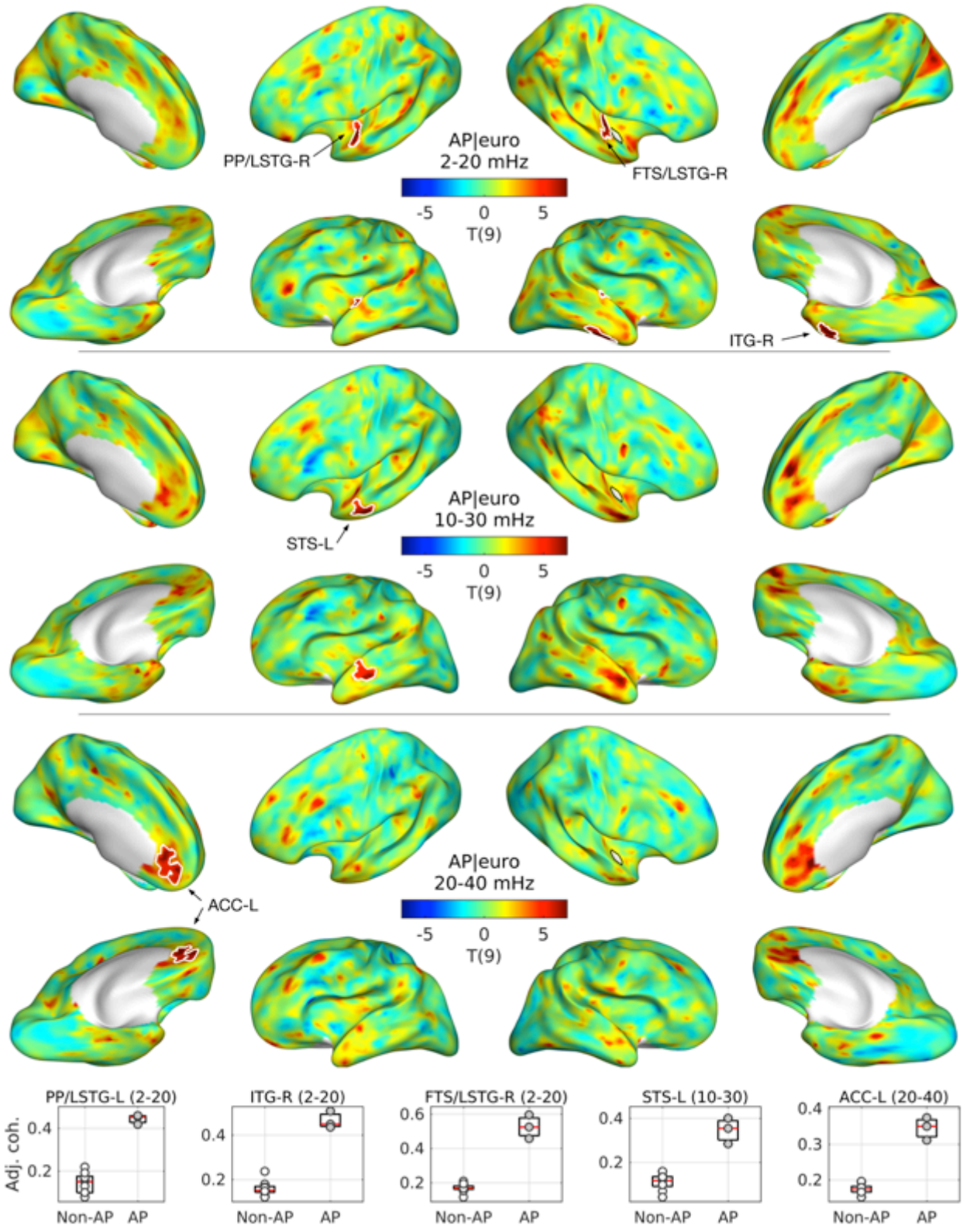

Figure S16. Effect of AP in cross-coherence only with European musicians. T-statistic maps are projected onto semi-inflated cortical surfaces. Significant clusters are indicated by white contours. Below the T-maps, boxplots with regression lines are given for the peak of each cluster. An open circle represents a musician without AP and a gray circle represents a musician with AP. Abbreviations: PP/LSTG-L, left planum polare and lateral superior temporal gyrus; ITG-R, right inferior temporal gyrus; FTS/LSTG-R, right first transverse sulcus and lateral aspect of the left superior temporal gyrus; STS-L, left superior temporal sulcus; ACC-L/R, left/right anterior cingulate cortex.

It is true that not all clusters were found from the GLM only with European musicians. However, because of the relationship between sample size and statistical power, it is not surprising that the GLM result with a subset detects less than one with a full dataset. While the discrepancy between the datasets could be either false positives or false negatives, the cortical regions related to the ventral auditory pathway (i.e., FTS/LSTG-R, PP/LSTG-L, ICSI-R, STS-L) were reliably found in both analyses as well as other cortices such as ACC-L, TIFG-L, of which the implication was discussed in the main text. Moreover, the similarities between the T-maps were very high (Pearson's correlation between 0.96 and 0.98). Therefore, although it was not possible to completely rule out the possibility of the confounding effect from ethnicity, given the evidence of the additional analyses here, we believe the confounding effect is reasonably controlled.